CHALMERS
UNIVERSITY OF TECHNOLOGY

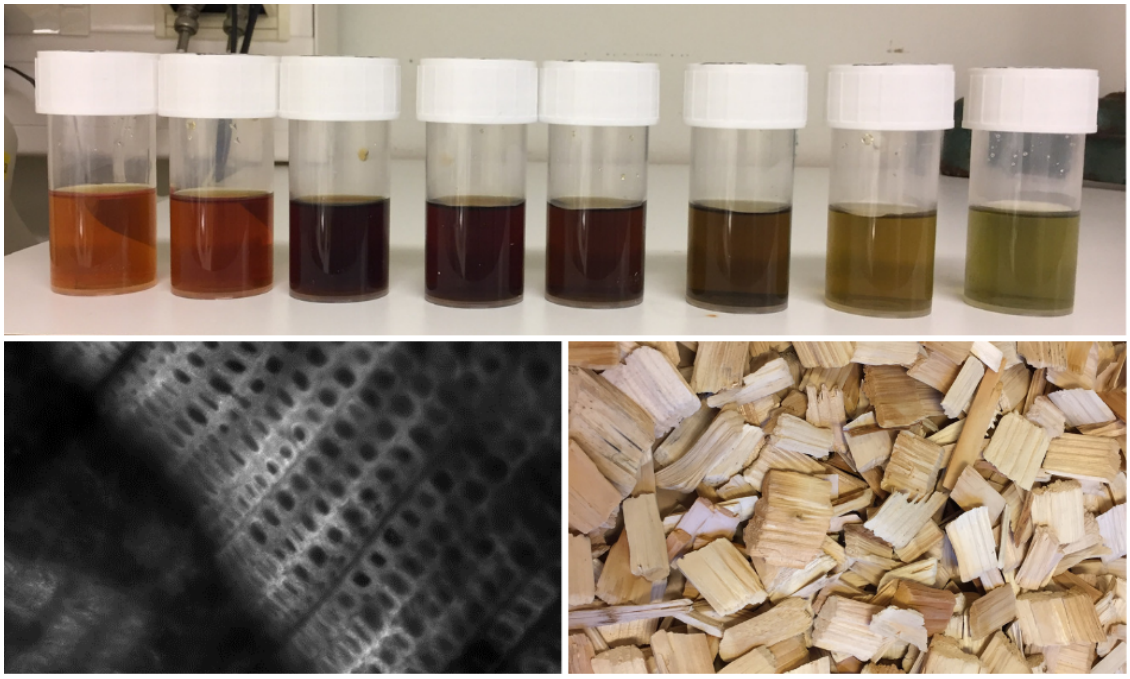

Kraft Cooking Kinetics

On the level of the fibre wall thickness

Master's thesis in Innovative and Sustainable Chemical Engineering

ANNA LIDÉN

Department of Chemistry and Chemical Engineering
CHALMERS UNIVERSITY OF TECHNOLOGY
Gothenburg, Sweden 2019

Master's thesis 2019

Kraft Cooking Kinetics

On the level of the fibre wall thickness

ANNA LIDÉN

CHALMERS
UNIVERSITY OF TECHNOLOGY

Department of Chemistry and Chemical Engineering
Division of Forest Products and Chemical Engineering
Chalmers University of Technology
Gothenburg, Sweden 2019

Kraft Cooking Kinetics
On the level of the fibre wall thickness
ANNA LIDÉN

SUPERVISORS
Prof. Hans Theliander (Chalmers)
EXAMINER
Prof. Hans Theliander

Master's Thesis 2019
Department of Chemistry and Chemical Engineering
Division of Forest Products and Chemical Engineering
Chalmers University of Technology
SE-412 96 Gothenburg
Telephone +46 31 772 1000

Cover: Photo collage by the author. Upper figure: Black liquor fractions, Lower left: Image of cell wall of saw mill chips of spruce using Confocal Laser Scanning Microscopy. Lower right figure: Chips of spruce

Typeset in LaTeX
Printed by [Name of printing company]
Gothenburg, Sweden 2019

Kraft Cooking Kinetics
On the level of the fibre wall thickness
ANNA LIDÉN
Department of Chemistry and Chemical Engineering
Chalmers University of Technology

Abstract

The Kraft process is the dominating pulping process and has been used since the end of the 19th century. It has been the subject of many studies and the reaction mechanisms of the major reactions has been thoroughly studied (e.g Sjöström (1993), Gellerstedt (2009*a*), Gierer (1980)). However, the effects of mass transport, desorption and solubility are often neglected when discussing the delignification kinetics. In recent studies performed on Scots pine (*Pinus Sylvestris*), Dang (2017) suggests that the rate determining step actually is mass transfer/solubility on the level of the fibre wall thickness. In the light of this, the impact of the fibre wall thickness was explored, using the same flow-through reactor as described by Dang (2017) using wood meal of spruce (*Picea abies*) with thicker (sawmill chips) and thinner (thinning material) cell walls. Three maximum cooking temperatures were evaluated; 148, 158 and 168°C. The ionic strength was kept consistent at $[Na^+]$=0.52 mol/kg solvent. The concentration of $[OH^-]$ and $[HS^-]$ were kept constant at 0.26 mol/kg solvent.

It was observed that larger lignin fragments required more time to pass through the thicker cell walls of the sawmill chips. Another observation was that the maximum molecular weight increased with temperature, which may be the result of condensation reactions and/or higher mobility. At given cooking chemical composition, no difference in delignification was noticed for 148 and 158°C. However, at 168°C and cooking times over 120 minutes, a higher degree of delignification could be observed for thinning material compared to the sawmill chips. After 120 minutes, the resulting lignin fragments formed by condensation reactions or originally in the wood matrix, may have reached a critical size, where the difference in diffusion rate becomes significant.

The sugar analysis showed that xylose and galactose were consistently found in higher concentrations in the pulp from saw mill chips. The sugar analysis also showed that mannose is rapidly degraded/dissolved, while xylose seemed to be more protected. Mannose did not seem to be affected by an increment of the cell wall thickness.

To summarize;the findings in this Master's Thesis suggest that the cell wall thickness might have an impact on the kraft cooking kinetics, but more research is required to establish the phenomena observed.

Keywords: flow-through kraft cooking, spruce, kinetics, lignin, condensation reactions,

Acknowledgements

It is common courtesy to thank people at the end of a great project, and until now, I have always been amazed by the large number of people that is mentioned in acknowledgements. As it is, I have a large number of people that made this thesis possible and who I would like to thank. First of all, I would like to thank everyone at the division of Forest Products and Chemical Engineering for all the help regarding the - sometimes troublesome - equipment and all the nice fika. However, there are a couple of people that deserves a special thanks:

Prof. Hans Theliander , my supervisor and examiner, for introducing me to the topic, interesting discussions and for believing in me and this project

Research Engineer Ximena Rozo Sevilla for ALL the help regarding the laboratory work and for always taking the time to help me

M.Sc Anders Ahlbom for answers to all my so many questions, fun company in the lab and great cooperation with the equipment

Lic. Joanna Wojtasz-Mucha for putting her heart into fixing the ion chromatography and for great cooperation with the laboratory equipment

Ph.D Parveen Deralia for the help with the ion chromatography

Research Engineer Katarina Logg for the help with the analysis of the cell wall structure

Mr Tresser even though we have never met, the experiments would not have been made possible without the fast delivery of spare parts to the reactor pump

Anna Lidén, Gothenburg, June 2019

Contents

Abbreviations

ASL	Acid soluble lignin
BL	Black liquor
CLSM	Confocal laser scanning microscopy
GPC	Gel Permeation Chromatography
KL	Klason lignin
LCC	Lignin-Carbohydrate Complexes
MeGlcA	4-O-methyl-D-glucuronic acid
MFA	Microfibril angle
MWD	Molecular weight distribution
PL	Precipitated lignin
SEC	Size exclusive chromatography

1
Introduction

The pulping industry plays a significant role in the Swedish industry. Not only is it producing pulp and paper products that are used on a daily basis, but it is also an important product for export. Around 85 % of the pulp produced is being exported (Skogsindustrierna 2018).

Pulp can be produced by chemical methods, mechanical methods or by a combination of both. Wood is the dominating raw material in the pulping industry. The most common pulping method is the Kraft pulping process. Kraft means "strength" in German, which is suitable since this method results in strong fibres. The Kraft process is a chemical method in which the wood chips are cooked in the digester in an alkaline cooking liquor at elevated temperatures (150-170 °C) to remove the lignin, the "glue" of the wood matrix, and to liberate the fibres. The pulp is taken out of the digester, continues along the fibre line and finally ends up as bleached or unbleached pulp. The dissolved organic material and spent cooking chemicals, referred to as black liquor, is transferred to the recovery cycle, where the latent heat of the dissolved organic material and the cooking chemicals are recovered.

Unfortunately, a lot of the carbohydrates in the wood are lost. This is because of degradation and dissolution in the alkaline environment, resulting in a relatively low yield. In a softwood kraft mill, the typical yield is only 45-55% (Sjöström 1993). The low yield is not beneficial from an economical point of view nor as it comes to material efficiency. An improved yield would give the possibility to reduce the amount of organic material in the black liquor, which could reduce the load of evaporators in the recovery cycle among others unit operations. Moreover, as the need for products from bio-based raw materials and biorefineries is becoming more and more pronounced, the importance of sustainable pulp mills is increasing.

The Kraft process has been used since the end of the 19th century, and has been the subject of many studies. It is a complex process, involving not only a complex raw material, but also heterogeneous reactions, mass and heat transfer. The reaction mechanisms of the major reactions have been thoroughly studied (e.g Sjöström (1993), Gellerstedt (2009*a*), Gierer (1980)) and are well documented. However, the effects of mass transport, desorption and solubility are often neglected when discussing the delignification kinetics. The rate determining step has in many studies been assumed to be the chemical reactions (Dang, Theliander & Brelid 2016). In recent studies performed on Scots pine (*Pinus Sylvestris*), Dang (2017) suggests that the rate determining step actually is mass transfer/solubility on the level of the fibre wall thickness. In the light of this, the impact of the fibre wall thickness will be explored by using the same flow-through reactor as described by Dang (2017) using sawmill chips and thinning material of spruce (*Picea abies*).

1.1 Aim

The overall aim of the Master's Thesis work is to gain further knowledge of the Kraft cooking kinetics. This will be done by investigating the impact of the cell wall thickness as suggested by the findings of Dang (2017), using thinning material (thin fibre wall thickness) and sawmill chips (thicker fibre wall thickness) of spruce.

The aim of the thesis is to answer:

What impact do the cell wall thickness have on the Kraft cooking kinetics?

This includes:

- Perform experiments using a small flow-through reactor cooking pulp with different cell wall thickness and evaluate the effect of temperature
- Analysis of lignin content, sugar content, molecular weight distribution and measurement of cell wall thickness

Further knowledge of the kinetics will give deeper understanding of the Kraft cooking, and possibilities for optimization.

1.2 Delimitation

Since the Master's Thesis is performed in a limited period of time, several limitations have to be made. These will be described in the following section.

- The Kraft cooking experiments will be performed in the small flow-through reactor, thus only on laboratory scale.
- The chips will be milled into wood meal to eliminate the effect of mass transport on a larger length scale. Hence, only the mass transport through the fibre wall will be studied.
- Only one wood specie will be used, namely spruce. The results will thus only be applicable for that particular specie. No general conclusions may be drawn.
- Concentration of OH^- and SH^- will be kept constant
- The ionic strength will be kept constant.
- Each cooking will be performed only once, with the exception of reruns
- Regarding the analysis of the black liquor and the wood residue, only carbohydrate and lignin content will be analyzed. Thus, no information regarding the content of ash or extractives is obtained.
- The content of Hexerunic acid and Rhamnose will not be analyzed

2

Theory

The following section will describe the basics of softwood, current knowledge of the Kraft pulping process and analytical techniques for analysis of wood.

2.1 Wood

Wood is the most abundant biomass on earth and it is also the most common material in the Kraft pulping industry. It may seem as a rather simple material, but its anatomy is complex and can be studied at many levels.

2.1.1 Softwood

Wood may be classified as *softwood* or *hardwood*. Sometimes larch wood is mentioned as a third category. Woods classified as softwood come from gymnosperms, while woods classified as hardwood come from angiosperm. The anatomy of the two differs. Softwood have a simpler anatomy, consisting of mainly one cell type, namely tracheids. The variation within different softwood species is rather small (Daniel 2009).

2.1.2 Wood structure

The structure of softwood will be explained in all four levels seen in Figure 2.1; macroscopic, microscopic, ultrastructural and molecular level.

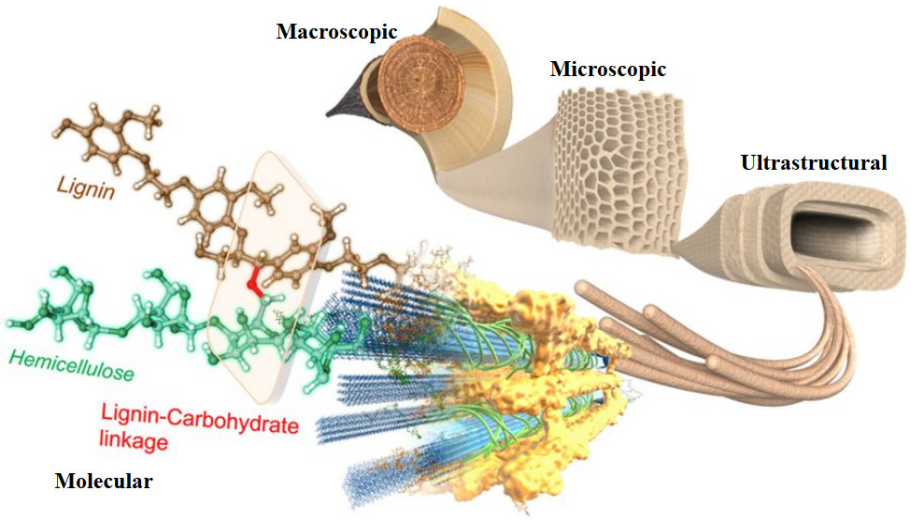

Figure 2.1: A model of the hierarchical structure of wood. Adapted from Nishimura et al. (2018)

2.1.2.1 Macroscopic

Starting at the largest scale, the macroscopic scale. A transverse section of the wood stem is seen in Figure 2.2.

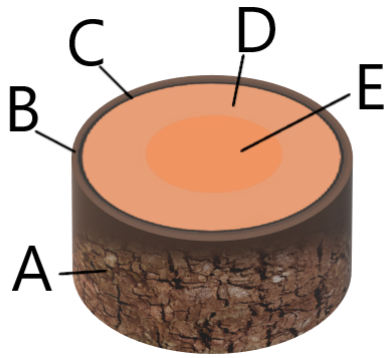

Figure 2.2: The transverse section of a wood stem.
a= outer bark, b=phloem, c= cambium, d= sapwood, e= heartwood

Bark is divided into outer and inner bark. The outer bark consists of dead cells and is for protection. The inner part, also called *phloem*, is living and its function transport downwards and storage of nutrients (Henriksson et al. 2009). Bark consists of 10-30% extractives, 15-45% cellulose, 15-40% lignin, depending on species. The remainder consists of tannins and other carbohydrates (Biermann 2012*b*).

Inside the phloem, a thin layer of cambium is present. Cambium is responsible for production new cells of phloem and xylem. Xylem is divided into sapwood and heartwood. The cells of sapwood are mostly dead, but a few cells are living. They provide transport of water and nutrients upwards. Heartwood consists of dead cells and its function is to act as support(Daniel 2009).

The inner part of the tree is called the pith. Closest to the pith, the wood tissue formed during the early years of the tree is formed. This is called *juvenile wood* and has different properties compared to the wood tissue formed during the later years, *mature wood*. For example, the fibres from juvenile wood are shorter (Henriksson et al. 2009).

2.1.2.2 Microscopic

Softwood has a much simpler cell type configuration compared to the hardwoods, concentrated to a limited number of cell types. A summary of the different cell types and their functions is found in Table 2.1.

Table 2.1: Summary of the cell types and their function in softwood

Cell type	**Function**
Tracheids	Conduction Support
Parenchyma	Storage Secretion of resins
Ray tracheids	Conduction

Tracheid is the dominating cell type in softwood and constitutes approximately 90-95% of the total cell volume (Fengel & Wegener 2011). One may also find tracheids in hardwood, but to a lesser degree. Moreover, the hardwood tracheids are shorter. The major functions of the softwood tracheids are conduction and support. Tracheids are slender fibres with squarish cross-section. Typical dimensions for spruce (*Picea Abies*) is a length between 1.1-6 mm and width between 21-40 μm (Daniel 2009). The dimensions vary depending on genetic factors and growth conditions (Sjöström 1993). If the water supply has to be large, e.g during spring, the tracheids will adapt and become thinner and longer to provide efficient water transport. This is known as *earlywood*. During periods when the water supply is not as important, the tracheids become thicker and shorter. This is referred to as *latewood*. The variation between earlywood and latewood is seen as annual rings. Conduction is also provided by the ray tracheids, oriented in radial direction.

The parenchyma cells are predominately arranged in radial direction, and are responsible for storage of nutrients and secretion of resins. They surround resin canals, which are intercellular spaces that forms a channel network within the tree. Resin canals are only present in softwoods (Sjöström 1993).

The different cell types are connected via pit pairs. Three kinds of pits exist; simple, half-bordered and bordered, see Figure 2.3. All pits consist of a pit membrane composed by the primary wall and middle lamella from the two cells connected (Sjöström 1993). Simple pits connect parenchyma cells, borded pits connect tracheids, and half-bordered pits connect tracheid with ray parenchyma.

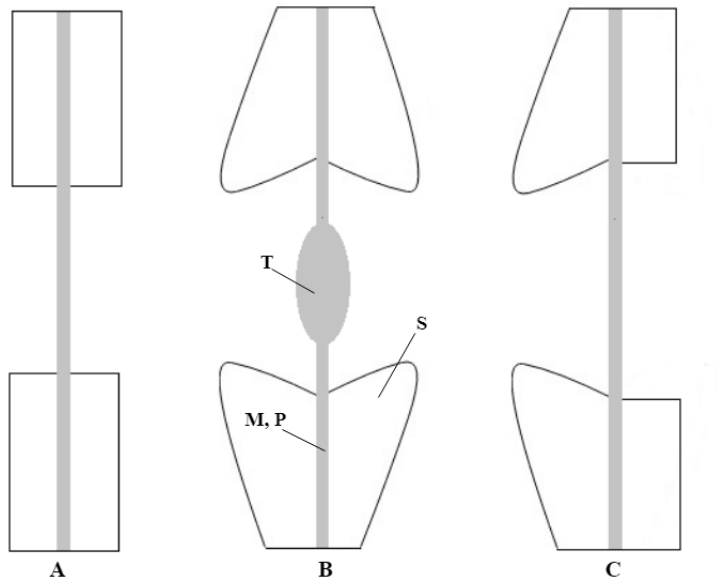

Figure 2.3: A. Simple pit pair, B. Borded pit pair, C. Half borded pit pair T= Torus, M= middle lamella, P = primary wall and S= Secondary wall

In softwood borded pit pairs, a central torus surrounded by a network of cellulose strands, *margo*, is found. The torus is rich in pectin and also contains cellulose (Sjöström 1993). When the torus is pressed against either side of the border, the cell is closed. This known as cell aspiration and happens for example during formation of heartwood (Daniel 2009)

2.1.2.3 Ultrastructure

Figure 2.4 shows the structure of the cell wall. The cells are held together by the middle lamella. Closest to the middle lamella, the primary wall is found. After the primary layer follows the secondary layer, which is composed by three layers: S1, S2 and S3. Lumen is the hollow center of the cell.

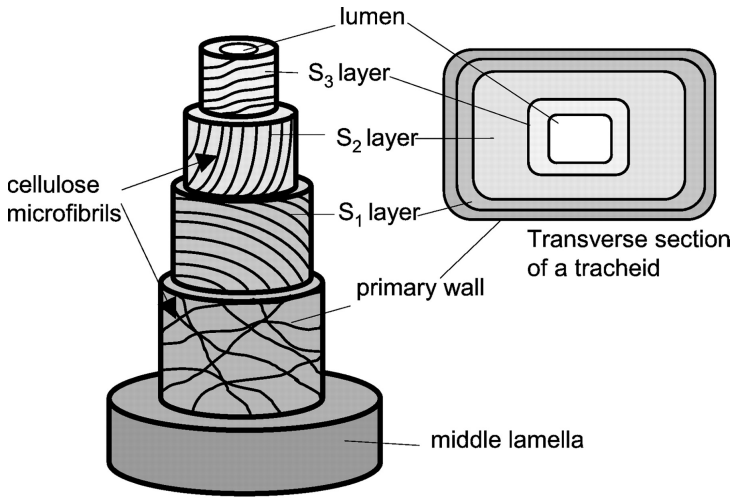

Figure 2.4: The transverse section of a tracheid and the cell wall structure.(Plomion et al. 2001) reprinted with permission

Cellulose, hemicellulose and lignin build up the several layers. The composition varies depending on species, early/late wood or juvenile/mature wood. The middle lamella has the highest lignin concentration (g/g) of the layers, but also contains pectin. Pectin can also be found in the primary layer together with hemicellulose and cellulose (Teleman 2009).

The arrangement of the cellulose fibrils in the layers differ. How the microfibrils are arranged is of great importance for the physical properties of the wood. The orientation can be either rotation around the cell axis to the right (Z-direction) or to the left (S-direction). In the primary layer, the cellulose microfibrils are oriented randomly. The microfibrils in the secondary layer are either in S or Z-direction, with varying microfibrilar angle (MFA) (Sjöström 1993).

Table 2.2 shows typical dimensions of the different layers. As can be seen, S2 is the dominating part of the cell wall. The varying thickness of S2 depends on whether it is early wood or late wood (Harada & Côté 1985).

Table 2.2: Typical cell wall thickness of the primary and secondary layers(Sjöström 1993)

	Thickness [μm]
Middle lamella	0.2-1
Primary wall	0.1-0.2
S1	0.2-0.3
S2	1-5
S3	0.1

2.1.2.4 Molecular

Cellulose, hemicellulose and lignin are the major constituents of the wood cell wall. The chemical composition of spruce (*Picea Abies*) is seen in Table 2.3.

Table 2.3: Chemical composition of spruce [% of dry wood weight]

	Literature data (Sjöström 1993) [% of dry wood weight]
Total extractives	1.7
Lignin	27.4
Cellulose	41.7
Glucomannan	16.3
Xylan	8.6
Other polysaccharides	3.4
Residual constituents	0.9

As seen in Table 2.3, spruce also constitutes minor amounts of other polysaccharides, extractives and inorganic materials. The inorganic material present is for example present as counterions to negatively charged carbohylgroups in hemicellulose (xylan) , pectin and extractives (Teleman 2009), (Sjöström 1993). Cellulose, hemicellulose and lignin and a brief description of other polysaccharides will be presented in the following section.

Cellulose
The main component of wood is cellulose. Aggregates of cellulose microfibrils are found in the cell wall. These have alternating crystalline and amorphous regions (Sjöström 1993), (Sun 2010). Cellulose is a linear homopolysaccharide consisting of D-glucopyranose units linked together by β-(1→4)-glucosidic bonds, seen in Figure 2.5. The degree of polymerization can be up to 15 000. Parallel cellulose chains form cellulose sheets. Between these sheets, it is probably strong hydrophobic interactions and van der Waals forces that acts (Henriksson 2009*b*).

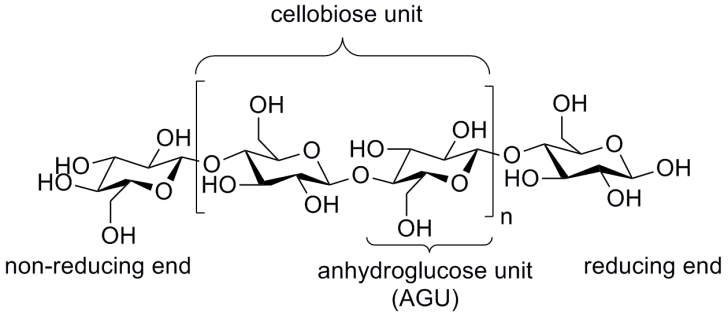

Figure 2.5: The structure of cellulose (Olsson & Westman 2013)

The combination of the glycosidic bonds and internal hydrogen bonds makes the cellulose structure stiff. The stiff structure, that allows close packing together with extensive intermolecular and intramolecular hydrogen bonds makes the cellulose impossible to dissolve in water or most organic solvents. It can however be dissolved in some ionic liquids (Sun 2010), (Henriksson 2009*b*).

The end groups of the cellulose have different properties depending on the position of the hydroxyl group, seen in Figure 2.5. The reducing end is the end with the hydroxyl group positioned on C1. The reason behind this is seen in Figure 2.6 when comparing C1 and C4. The anomeric carbon (C1), i.e the carbon carrying the aldehyde functionality, is not "locked" like C4, but can instead be easily rearranged. The hydroxyl group at the other end of the cellulose chain is positioned at C4 and does not show the same reducing properties. This is referred to as the non-reducing end group (Fengel & Wegener 2011). Under alkaline conditions and high temperature, the reducing end group is rearranged, leading to elimination of the end group. The peeling reaction proceeds until stopping reaction occur after approximately 65 monomers have been peeled off (Henriksson 2009*b*).

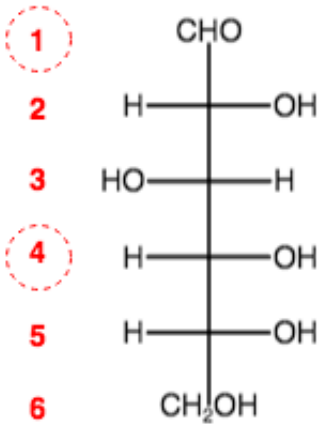

Figure 2.6: Carbon number 1 is the reducing end since it is not locked in a glycosidic bond like carbon number 4, and can easily be rearranged

Hemicellulose
Unlike cellulose, hemicelluloses are generally heteropolysaccharides. The degree of polymerization of hemicelluloses is lower than that of cellulose and its backbone may be branched. In addition to this, hemicellulose is amorphous, which makes it more susceptible to chemical reactions than cellulose (Basu 2018). Moreover, the hemicellulose content varies a between softwood and hardwood.

(Galacto)glucomannan
The Galactoglucomannans are the major hemicelluloses of softwood and compose approximately 20 % of the hemicellulose content (dry weight). (Galacto)glucomannans consist of linear chains of β-(1→4)-D-mannopyranosyl units and β-D-glucopyranosyl residues attached by α-(1→6) linkage, see Figure 2.7. The galactoglucomannans can be divided into two fractions in softwood, depending on the ratio of galactose:glucose:mannose. Galactoglucomannan has a ratio of 1:1:3, while glucomannan has 0.1:1:3 (Sjöström 1993), (Teleman 2009).

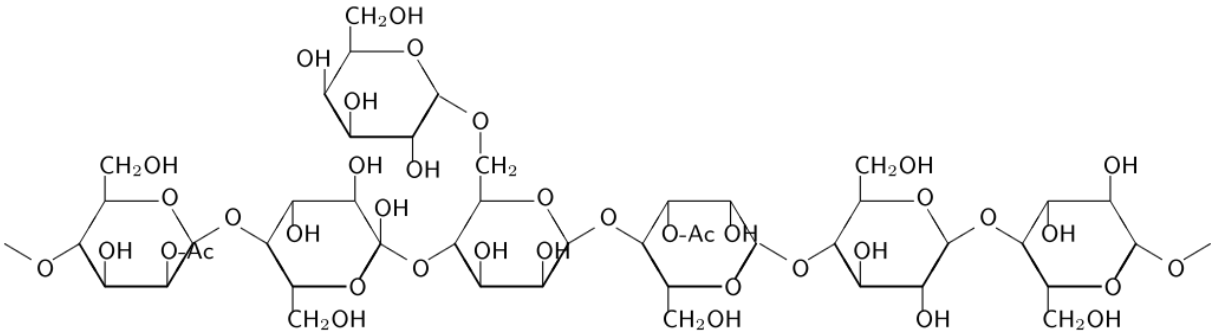

Figure 2.7: The strucuture of Galactoglucomannan

Under alkaline conditions, the acetyl groups are easily cleaved. Alkaline conditions cause alkaline hydrolysis and combined with high temperatures it also results in extensive peeling.

(Arabinoglucorono)xylan
Softwood is composed by about 5-10 % (w/w) arabinoglucoronoxylan (Sjöström 1993). Its structure is found in Figure 2.8. The backbone consists of β-(1→4)-D-xylopyranosyl residues. 4-O-methyl-D-glucuronic acid (*MeGlcA*) may be linked to the backbone with α-1,2 linkage. Softwood xylan also carries α-L-arabinofuranose to position C3.

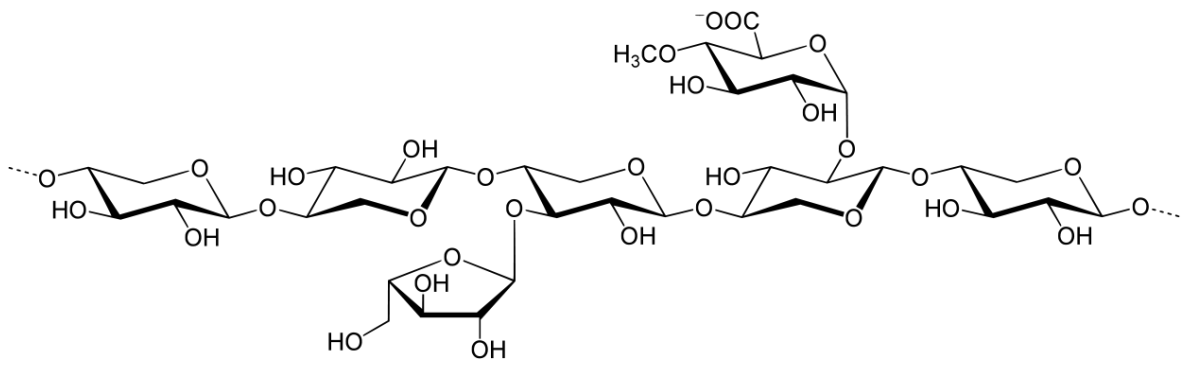

Figure 2.8: The structure of Arabinoglucoronoxylan

Compared to the hardwood xylan, softwood xylan contains no acetyl groups and has a higher degree of MeGlcA. MeGlcA is degraded under alkaline conditions and looses as hydrogen atom. A methoxyl group may be eliminated as methanol, resulting in the formation of hexenuronic acid (Gellerstedt 2009*a*).

As with the glucomannans, deacetylation easily occurs under alkaline conditions. However, peeling reaction is prevented to some extent due to the presence of the side groups (Teleman 2009). At low temperatures, the MeGlcA prevents the peeling reaction. The arabinose on C3 is eliminated from the xylan backbone during the peeling, under simultaneous formation of metasaccharinic acid end group. This stabilizes the chain against further peeling (Sjöström 1993).

Studies by Wigell et al. (2007) on softwood suggests a close relationship between xylan and lignin, due to the xylan degradation being practical proportional to the delignification. Wigell et al. (2007) also showed that xylan was not significally affected by primary peeling. Another reason why the yield of xylan is higher than that of glucomannan is because of readsorption of xylan on the cellulose fibres (Yllner & Enström 1956).

Other polysaccharides

The main types of carbohydrates in wood are cellulose and the hemicelluloses described above. However, small amounts of other carbohydrates such as arabinogalactans, galactan, arabinan, other pectic material and starch (amylose and amylopectin) are also present in the wood matrix. The most common monomers in these constituents are galactose, arabinose and rhamnose (Sjöström 1993).

The backbone of arabinogalactan consists of galactose units linked together by β-(1$\rightarrow$ 3) linkages and β-(1$\rightarrow$ 6) linked side chains of galactose, arabinose and glucuronic acid. Studies by Willfor & Holmbom (2004) suggest that the ratio of galactose:arabinose:glucuronic acid is 3.6:1:0.8. Arabinose can also be found in the backbone of the highly branched arabinans. The arabinose units are joined by α-(1$\rightarrow$ 5) linkages and have side chains of arabinose units linked by α-(1$\rightarrow$ 3) linkage (Fengel & Wegener 2011). The backbone of the galactans is composed by β-(1$\rightarrow$ 4)-linked galactose units and is partially substituted with a side group of galacturonic acid (Teleman 2009).

Lignin

Lignin works as the "glue" in the wood cell, holding different cell wall components together. Other attributes lignin introduces to the cell wall include hydrophobicity, stiffness and protection against microbial degradation. The reason why lignin can work as protection against microbial degradation is because it makes the wood tissue so dense that the polysaccharide degrading polymers cannot enter (Henriksson 2009*a*).

Lignin is a large bioploymer with a more complex structure than cellulose and hemicellulose. It is neither linear, nor branched. Instead, lignin is like a three dimensional web built up monomers, so called monolignols. There are mainly three monlignols; p-coumaryl alcohol, coniferyl alcohol and sinapyl alcohol, seen in Figure 2.9. Softwood lignin consists mostly of Coniferyl alcohol, small amounts of p-Coumaryl alcohol, but no Sinapyl alcohol.

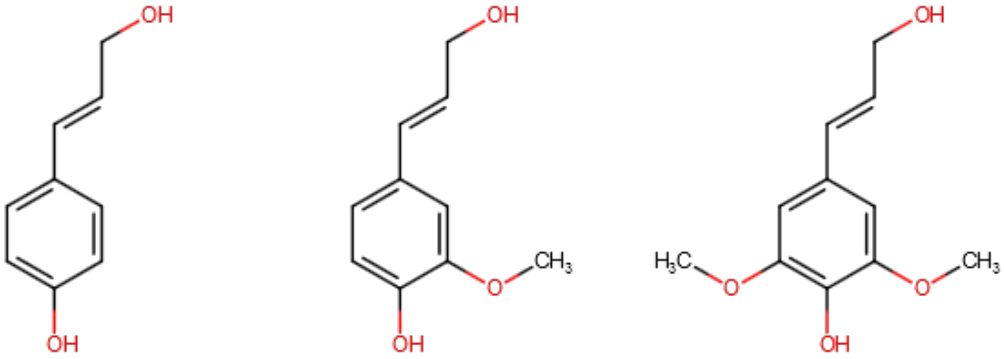

(a) p-coumaryl alcohol *(b) coniferyl alcohol* *(c) sinapyl alcohol*

Figure 2.9: The structure of the three most common monolignols

The monolignols are connected by carbon-carbon bonds (C-C) as well as ether bonds (C-O-C), seen in Figure 2.10. Studies Erickson et al. (1973) on spruce showed that the most common bond is β-O-4, but other linkages such as α-O-4, β-β and 5-5 etc. occur as well, see Table 2.4.

Table 2.4: The frequency of common linkages in lignin per 100 C_9 units in spruce (Erickson et al. 1973)

Type of linkage	*Frequency*
β-O-4	49-51
α-O-4	6-8
β-5	9-15
β-1	2
5-5	9.5
4-O-5	3.5
β-β	2

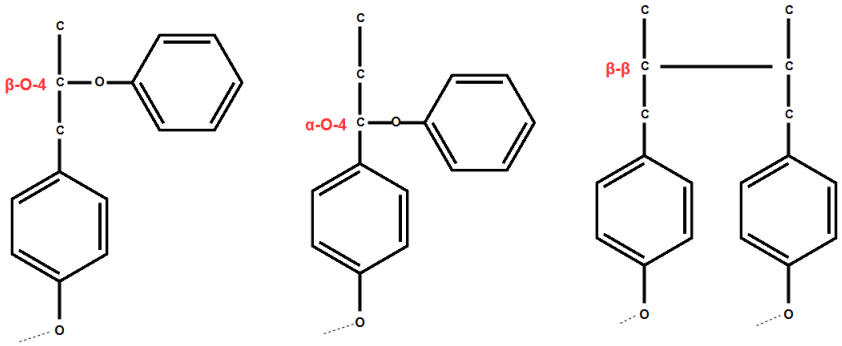

Figure 2.10: β-O-4, α-O-4 and β-β bonds connect monolignols

Covalent bonds between lignin and the polysaccharides in the wood matrix are also present. These are called "Lignin-carbohydrate complexes" (*LCC*) (Deshpande et al. 2018) (Nishimura et al. 2018). Lawoko et al. (2005) suggested that softwood lignin is part of two kinds of LCC of different structures; one that is attached to xylan and one to (galato)glucomannan.

2.1.3 Sawmill chips and thinnings

Sawmill chips come from the outer part of the tree and is the residual material that remains when a log is sawed into boards. Since they come from the outer part of the tree, they contain a high degree of mature wood. Mature wood has a high degree of long fibres and high density (Henriksson et al. 2009).

In order to improve the quality of the forest it is important that the right selection of trees is felled. This cutting is referred to as thinning and the the wood felled is the main wood supply to pulp and paper industry (Henriksson et al. 2009). This wood has a large portion of juvenile wood, which means that the fibres present are shorter and thinner compared to the sawmill chips.

2.2 Kraft pulping

The most common pulping process today is the Kraft process. The Kraft process has been used since the end of the 19th century and it is known for its strong pulp and excellent chemical recovery. A simplified flow chart of the Kraft pulping process is seen in Figure 2.11.

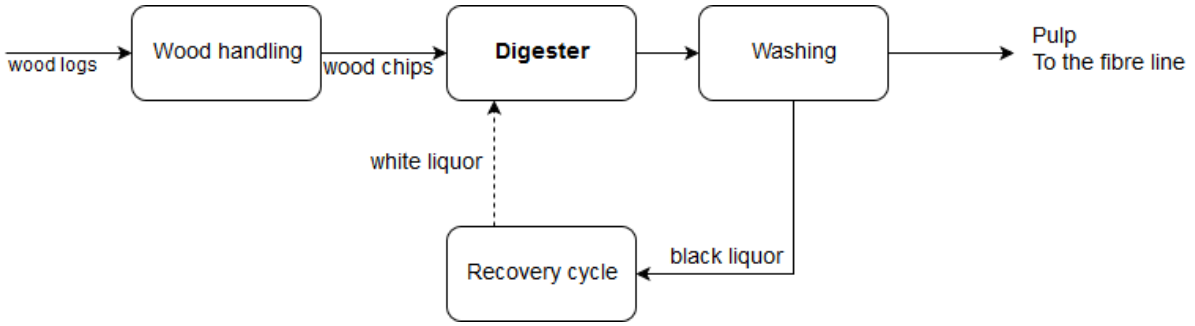

Figure 2.11: Simplified flow chart of the Kraft pulping process

The logs enter the wood yard, where they are debarked, washed and chipped into proper size before entering the digester. The digester is the core of the Kraft pulping process. This is where the cooking liquor, referred to as white liquor, active chemicals sodium hydroxide and sodium sulphide, is introduced. Via actions of the active cooking chemicals, the wood matrix is delignified and, unfortunately, some carbohydrates are degraded. The digester operates normally at elevated temperatures, around 150-170°C for 0.5-3h (Biermann 2012*b*), (Sjöström 1993). However, prior to the delignification, the chips are steamed and impregnated with white liquor. The purpose of the steaming is to remove air entrapped inside the lumen and to preheat the chips. After the steaming, the wood chips are impregnated with the white liquor to swell the fibre walls and thereby make the wood matrix more accessible to the cooking chemicals. The delignification kinetics and the chemistry in the Kraft cooking are explained in section *2.2.1 Kraft cooking*.

The pulp is taken out of the digester and continues along the fibre line with washing, screening, and if bleached, oxygen delignification and bleaching to remove the last portion of lignin. The dissolved organic material and spent cooking liquor, referred to as black liquor, is transferred to the recovery cycle, where the black liquor is evaporated and incinerated, resulting in a smelt and high pressure steam. The smelt is dissolved to green liquor and is by causticizing recovered as the active cooking chemicals in the white liquor, and transferred back to the digester.

2.2.1 Kraft cooking

The main goal with the Kraft cooking is to remove the lignin and to liberate the fibres. In order to achieve this, three actions must happen according to Bogren (2008):

- Fragmentation of lignin
- Solubilization of lignin
- Transport of soluble lignin fragments to the bulk liquor

The fragmentation and solubilization is achieved by reactions of lignin with the active cooking chemicals in the white liquor; hydroxide ions and hydrosulphide ions. The active ions may be formed according to Equation 2.1, when sodium sulphide is dissolved in water.

$$Na_2S + H_2O \rightarrow 2Na^+ + OH^- + HS^- \tag{2.1}$$

However, the cooking chemicals are consumed by reactions with the carbohydrates as well. The approximate consumption of alkali during the Kraft cooking of softwood is listed below (Chiang et al. 1987):

- **15kg/ton wood** Deacetylation
- **60 kg/ton wood** Neutralization of carbohydrate degradation products
- **35kg/ton wood** Peeling reactions

2.2.1.1 The chemistry of kraft cooking

The chemical reactions of lignin and the carbohydrates taking place during the Kraft cooking have been thoroughly studied (e.g (Sjöström 1993), (Gellerstedt 2009*a*), (Gierer 1980)).

Reactions of lignin
According to Gierer (1980), there are two kinds of delignifications reactions; degradation reactions and condensation reactions. The degradation reactions lead to the desired fragmentation and solubilization of the lignin, while the condensation reactions on the opposite lead to an increment of the lignin molecular weight and precipitation.

The delignification reactions have been thoroughly studied (Gierer (1980); Gellerstedt (2009*a*); Sjöström (1993)). The main chemical reactions have been clarified to be:

- Cleavage of β-aryl and α-aryl ether linkages in phenolic and non-phenolic structures
- Demethylation reactions
- Condensation reactions

β-aryl ether linkages are the most abundant bonds and cleavage of these are therefore of great importance for the degradation reactions. Reaction of phenolic β-O-4 structures is an efficient reaction thanks to the presence of HS^-. If no HS^- is present, an alkali stable enol is formed, and no fragmentation will occur via the phenolic β-O-4 structures. The reaction path leading to fragmentation is seen in Figure 2.12.

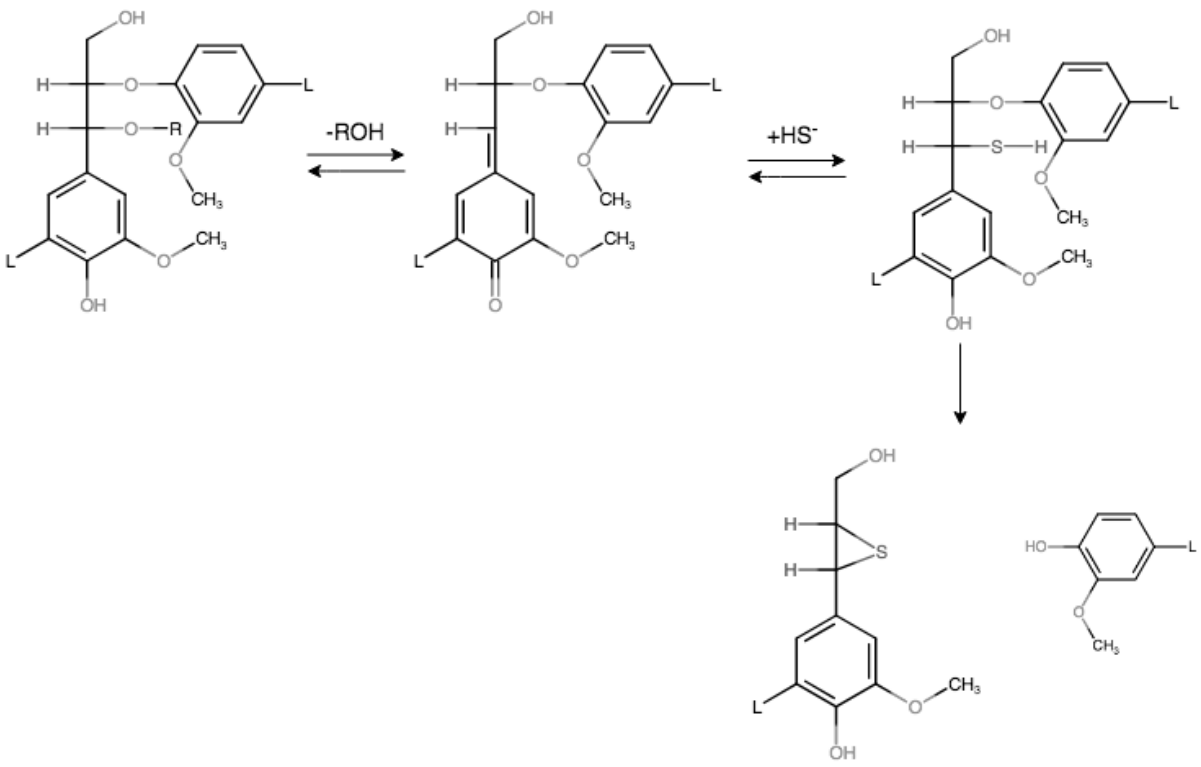

Figure 2.12: A simplified schematic figure of one of the routes of the reaction of the phenolic β-O-4 structures

Non-phenolic β-O-4 structures can be cleaved as well, see Figure 2.13. This cleavage does not involve HS^-. Instead, it is only dependent on ionization of α-hydroxyl groups. A non-stable epoxide and a new phenolic lignin end group are formed when a nucleophilic attack occurs. This is a rather slow reaction, compared to the cleavage of phenolic β-O-4 structures, and is dependent on the concentration of OH^- (Gellerstedt 2009*a*).

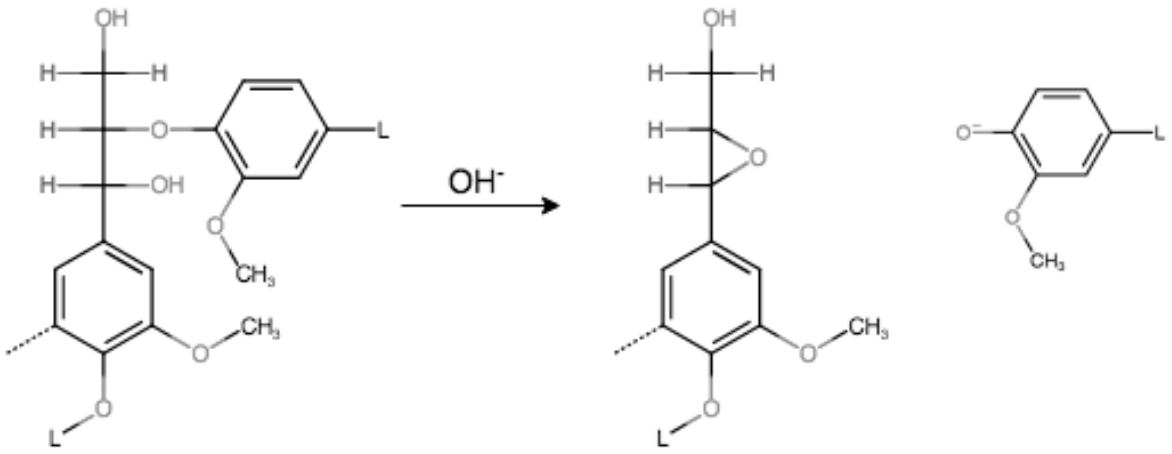

*Figure 2.13: Reaction of nonphenolic β-O-4 structures. Redrawn from (Gellerstedt 2009*a*)*

Another type of lignin reaction is undesired condensation reactions. According to Sjöström (1993), a variety of condensation reactions are known to occur in Kraft pulping. Carbon-carbon linkages are formed between the lignin entities during the cook, which might be the result of condensation reactions. These reactions retard the delignification.

Demethylation of lignin may also occur. This is caused by the action of HS^-, which results in formation of methyl mercaptan, see Figure 2.14. Methyl mercaptan may be oxidized to dimethyl disulfide in the presence of air. Both methyl mercaptan and dimethyl disulfide are highly volatile and malodorous compounds (Sjöström 1993). As seen in Figure 2.14, the attack can also be perfomed by a methylmercaptide anion, formed under the alkaline conditions. This attack leads to the formation of the malodorous compound dimethylsulfide (Gellerstedt 2009*a*).

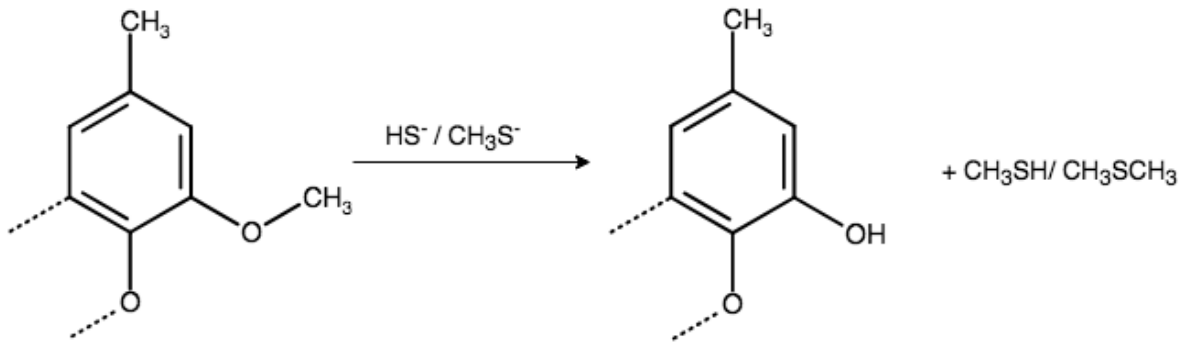

Figure 2.14: Methylmercaptan or dimethylsulfide may be formed when hydrogen sulfide or a methylmercaptide anion attacks an aromatic methyl ether group

Reactions of carbohydrates

It is not only lignin that is affected by the cooking chemicals. Unfortunately, the high temperature and alkaline environment in the digester cause fragmentation and dissolution of the carbohydrates present in the wood matrix. The hemicelluloses are more susceptible than cellulose, due to their amorphous structure and lower molecular weight. The hemicelluloses are attacked at lower temperatures and to a higher extent.

During the initial phase of the cook, the acetyl groups of the hemicelluloses are deacetylated and split off. At a temperature around 100°C the primary peeling reaction starts. The reducing end group will form an equilibrium between hemiacetal and the open aldehyde form in the aqueous environment of the cooking liquor (Gellerstedt 2009*a*). The peeling reaction starts by the rearrangement of the reducing end, resulting in β-elimination. The liberated product created by the β-elimination may react further to an isosaccharinc acid, which ends up in the black liquor. The peeling reaction occurs until the stopping reaction occurs after approximately 65 monomers have been peeled off and the polysaccharide is stabilized (Brännvall 2009). A simplified schematic figure of the peeling reaction is seen in Figure 2.15.

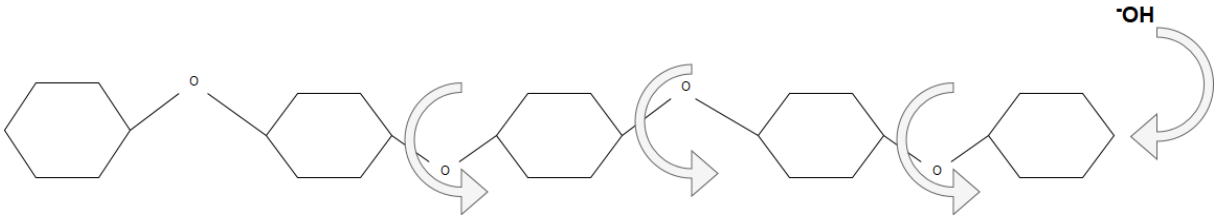

Figure 2.15: A simplified schematic figure of the peeling reaction. Redrawn from (Brännvall 2009)

During the peeling reaction, the degree of polymerization of the carbohydrates decreases. The result of the depolymerization may be a complete dissolution of the carbohydrate before it is further degraded. Aurell (1965) found that (galacto)glucomannans are especially sensitive to degradation and dissolution even during the heating up period of 110 °C. This is due to their amorphous structure and low degree of polymerization. As mentioned in *2.1.2.4 Molecular level*, xylan is prevented against peeling reaction due to the presence of sidegroups. When arabinose at position C3 is peeled off, it results in stabilisation of the polysaccharide chain and formation of stable metasaccharinic acid. This kinetic path may also happen to (galacto)glucomannans and cellulose (Gellerstedt 2009*a*).

The peeling reaction is one of the two major reactions of the carbohydrate during Kraft cooking. The other reaction is alkaline hydrolysis. Alkaline hydrolysis starts when the temperature rises above 150°C. During alkaline hydrolysis, the carbohydrate chain is randomly cleaved, giving rise to new reducing end groups and the opportunity for secondary peeling (Fengel & Wegener 2011).

2.2.1.2 Delignification kinetics

The delignification kinetics are very complex and the delignification involves several mechanisms; chemical heterogeneous reactions, heat and mass transport, sorption and solubility (Mattsson et al. 2017). These phenomena make the delignification kinetics difficult to model.

The course of events of the mentioned mechanisms:

1. Mass transfer of chemicals from bulk to surface of the chip
2. Mass transfer of chemicals from the surface of the chip to the reaction site (through pore system and cell wall)
3. Reaction and dissolution of wood components
4. Mass transfer of dissolved wood components from the reaction site to the surface
5. Mass transfer of dissolved wood components from the surface to the bulk

A frequently used description of the delignification of well impregnated wood chip is the "three phase model". This model describes the deliginification as pseudo-homogeneous reaction with an initial phase, a bulk phase and a residual phase, by plotting the decrease in delignification against the reaction time (Brännvall 2009).

The initial phase takes place below temperatures of 140°C and is characterized by fast dissolution of lignin. Gierer & Noren (1980) suggested that it is predominantly α- and β-aryl ether bonds in phenolic phenylpropane structures that are cleaved in this phase. The initial phase is followed by the bulk phase, where the majority of the lignin is removed. The fragmentation of lignin is achieved by cleavage of β-aryl ether linkages in phenolic and non-phenolic units (Gierer & Noren 1980). After the bulk phase, the slow residual phase takes place. The selectivity towards dissolution and degradation of lignin is very poor in this phase, and should be minimized (Brännvall 2009), (Sjöström 1993). The reason behind the slow delignification has been the subject of many research (e.g Lindgren & Lindström (1996), Gellerstedt et al. (2004), Evstigneyev (2019)). One reason behind the low reactivity may be because of condensation reactions of the lignin as suggested by Gellerstedt et al. (2004). Another explanation to the slow delignification of the final stage, given by Evstigneyev (2019) is that the absence of hydroxyl groups adjacent to the β-O-4 bonds in some of the side chains of the residual lignin. The essence of the LCCs during the final part of the delignification was pointed out by Lawoko et al. (2003), who found that the majority of the residual lignin (90 %) of softwood kraft pulp was chemically bound to carbohydrates.

The three phase model is a traditional way of describing the delignification process, but it is debated whether this is an accurate description from a mechanistic perspective or not (R. Obst 1983). However, this is not the only model for describing the delignification kinetics. Several models exist, more or less advanced. A well-known simplified model is the "H factor model" (Vroom 1957). In this model, the temperature and time are combined into a single variable to represent the extent of the cooking. Assumptions made include the assumption that the deliginification is a pseudo-homogeneous first order reaction and that the active cooking chemicals are constant. It is important to remember that the model is only valid for a certain wood specie, chip size and cooking chemical composition.

2.2.1.3 The effect of temperature

Temperature is an important parameter of the Kraft cooking kinetics. The delignification is highly dependent on this parameter and increases with increasing temperature. A temperature increase of 10°C results in a two fold increase of the delignification (Brännvall 2009). Dang (2017) evaluated the delignification at three different temperatures (148, 158 and 168°C) and did, not surprisingly, conclude that a higher temperature resulted in a higher degree of delignification. However, the residual phase lignin is reported not to be affected by an increased temperature in softwood kraft cooking for temperatures above 150 °C (Chiang et al. 1990).

Increasing the temperature also results in an increased loss of carbohydrates. The temperature has a significant effect on the alkaline hydrolysis and increasing the temperature will result in increased alkaline hydrolysis (Brännvall 2017). Moreover, studies by Nieminen et al. (2014) show that the secondary peeling increase with temperature for galactoglucomannan and xylan. The primary peeling of glucomannan is very fast even at 100 °C. Moreover, the primary peeling of xylan does increase with temperature.

2.3 Analytical techniques for analysis of wood

Wood is an anisotropic and heterogeneous material with inherent complexity and inaccessibility. This makes analysis of wood challenging.

2.3.1 Determination of the cell wall thickness

Confocal laser scanning microscopy (CLSM) is widely used in life science to study the distribution and structure of biological systems. This method can also be applied when studying the cell wall thickness of wood. The principle behind the image formation in CLSM is illumination of a sample containing flourescent constituents with one (or several) focused beam of laser. Light with lower wavelengths is emitted and detected, while radiation is absorbed.

Some of the advantages with CLSM is that it is non-destructive and can generate high quality images at micron level. Moreover, since lignin is auto-flourescent it is suitable to use this method.

2.3.2 Determination of lignin

Separating lignin is challenging in many ways. All analytical methods involve chemical changes of the lignin, since the lignin needs to be fragmented into soluble and analyzable fractions.

2.3.2.1 Determination of Klason lignin and Acid Soluble Lignin

Lignin may be isolated using acid hydrolysis. Acid hydrolysis can e.g be preformed according to method described by Theander & Westerlund (1986), where the solid wood residue or BL fraction is mixed with 72% sulfuric acid to a pH of 1-1.5, warmed in water bath, followed by dilution and hydrolysis at 125°C in autoclaves, filtration and drying. The result of acid hydrolysis will be a precipitate of condensed lignin (Klason Lignin) and a solution of monosugars and acid soluble lignin (ASL) (Biermann 2012*a*). However, not all carbohydrates may be hydrolyzed and dissolved in the acid hydrolysis, and some may remain in the filter cake (Gellerstedt 2009*b*). The Klason lignin is measured gravimetrically, while ASL is measured by ultraviolet microscopy (UV).

UV
UV spectroscopy is a technique used for analyzing aromatic or conjugated systems. The principle behind UV spectroscopy is the excitation of molecules to another electronic energy level. This is achieved by passing light through the sample at an appropriate wave length (200-400 nm), giving rise to absorption of the light (Bhattacharya Sati et al. 2011). Since lignin has an aromatic structure and conjugated double bonds, UV spectroscopy is a suitable tool for analyzing the lignin content.

The absorbance of the filtrate is measured at 205 nm. Degradation products from the polysaccharides are known to influence the absorbance at 280 nm and should therefore be avoided (Fengel & Wegener 2011). The content of ASL can be calculated by the use

of Lambert Beer's law, see Equation 2.2.

$$A = \varepsilon \cdot l \cdot C \tag{2.2}$$

Where A is the absorbance, l is the length of the cuvette [cm], C is the concentration of acid soluble lignin [g/L] and ε the molecular absorptivity [L $g^{-1}cm^{-1}$](Lin & Dence 1992).

2.3.2.2 Determining the molecular weight distribution of lignin

Lignin may be isolated using acid precipitation. The isolated lignin can be analyzed by gel permeation chromatography (GPC) to gain information about the molecular weight distribution (MWD).

GPC
GPC is sometimes referred to as size exclusive chromatography (SEC) and is a separation method based on the size of the solutes. The dried lignin precipitates may be dissolved in a solution of LiBr in DMSO and then injected into a porous gelled column. Molecules of smaller size will be retained for a longer time inside the column, since they are easily entrapped inside the porous structure. Larger molecules will not pass through the small pores and will be eluated earlier.

From the MWD, the average molecular weight can be calculated in three different ways; the weight average molecular weight (M_w), the number average weight (M_n) and the viscosity average molecular weight (M_v)(Bhattacharya Sati et al. 2011). The polydispersity, PD, is calculated as M_w/M_n. If PD is close to 1, it means that the mass of the molecules is rather uniform. If PD »1, it means that there is a non-uniform molecular mass.

2.3.3 Determination of carbohydrates

The content of carbohydrates is commonly determined by analyzing the monosugars in the filtrate that is obtained after acid hydrolysis. The detection of monosugars can be done by using high performance anion exchange chromatography coupled with pulsed amperometric detection (HPAEC-PAD).

HPAEC-PAD
HPAEC-PAD utilizes the fact that some neutral sugars actually are weak acids, with a pKa around 12. At high pH the sugars are ionized and separation may be achieved using a strong anion-exchange stationary phase (Rohrer 2013).

When the sugars have been separated, they are detected. UV/Vis is not a suitable choice of detector, since the mono- and oligosaccharides lack chromophores. A more suitable detector is PAD, in which the carbohydrates are oxidized on the surface of a nobel metal electrode. A waveform with different potentials is repeatedly applied to the electrode and the current that arises from the oxidation on the metal surface is being measured (Mechelke et al. 2017). Fucose may be used as an internal standard for quantification.

3
Material & Methods

The following section will explain the raw materials and the methods used, including cooking, analysis and measurement of cell wall thickness. Regarding the cooking and analysis, same methods as described by Dang (2017) will be used to be able to compare the results.

3.1 Raw material

Södra provided the sawmill chips and thinning material of spruce used as substrate in the experiments. Figure 3.1 shows the chips of both materials. The chips were dried in room temperature for a week, after which they were milled to a fine meal using a *Wiley wood mill* equipped with a sieve (<1mm). The wood meal was stored in room temperature to obtain a uniform moisture content. The moisture content of the wood meal used was measured by *Moisture Analyzer Sartorius MA 30* in connection with the cooking experiments. The moisture content of the wood meal was 92 ± 0.24%.

(a) Sawmill chips of spruce *(b) Thinning material of spruce*

Figure 3.1: The substrates used in the following experiments were prepared from sawmill chips and thinning material of spruce

3.2 Measurement of the cell wall thickness

The wood chips were cut to uncover the tranverse section, into smaller pieces with a thickness < 0.6 mm and a width < 9 mm. Determination of the cell wall thickness was done at Chalmers Material Analysis Laboratory using a *Nikon Ti-E/A1+* confocal laser scanning microscope equipped with two detector units; one four detector unit and one tunable emission detector unit (GaAsP detector). To avoid shrinkage of the fibre wall, the sample was analyzed wet. The data was analyzed using *Fiji ImageJ version 2.0.0-rc-59/1.51n.*

3.3 Preparation of cooking liquor

The cooking liquor was prepared by dissolving $Na_2S{\cdot}XH_2O$ in water. However, since the Na_2S contained an unknown amount of crystal water, ABC titration was performed to determine the concentrations of OH^- and SH^- in the cooking liquor (Biermann 2012*b*). The A and B steps of the ABC titration were performed by *Titroline®7000.*

$Na_2S{\cdot}XH_2O$ was dissolved in H_2O. Four samples of 10 g were taken from the original cooking liquor and titration followed according to the method described below.

(A) Prior to the first titration, an excess of $BaCl_2$ (200 g/L) was added to precipitate the carbonate anions. HCl 1M was by titration added until the titration point occured at pH 11. The amount of acid added, the "A-value", corresponded to all of the NaOH and half of the Na_2S. All of the Na_2S is converted to NaHS in water, with liberation of NaOH.

(B) An excess of formaldehyde (phenolphtalein and NaOH) was added to convert the NaHS to NaOH, according to Equation 3.1.

$$HS^- + CH_2O + H_2O \rightleftharpoons CH_2(OH)SH + OH^- \tag{3.1}$$

The release of NaOH caused a rise of the pH. The solution was once again titrated with HCl 1M until the titration point, when colour change was noted by the phenolphthalein. The amount of acid added, the "B-value", corresponded to half of the initial Na_2S.

The additional amount of water needed to obtained the desired concentrations of $[OH^-]$, $[SH^-]$ and $[Na^+]$ was calculated according to Appendix A. The initial composition of the cooking liquor was the same in all the cookings, namely $[OH^-]$ and $[SH^-] = 0.26$ mol/kg solvent and $[Na^+] = 0.52$ mol/kg solvent.

3.4 Flow-through reactor

The experiments were performed using a small flow-through reactor, described by Bogren et al. (2009), see Figure 3.2 and 3.3. The system consisted of a column (300x7.8mm) with coils of piping at both inlet and outlet. A high pressure pump was used to pump the cooking liquor through the system.

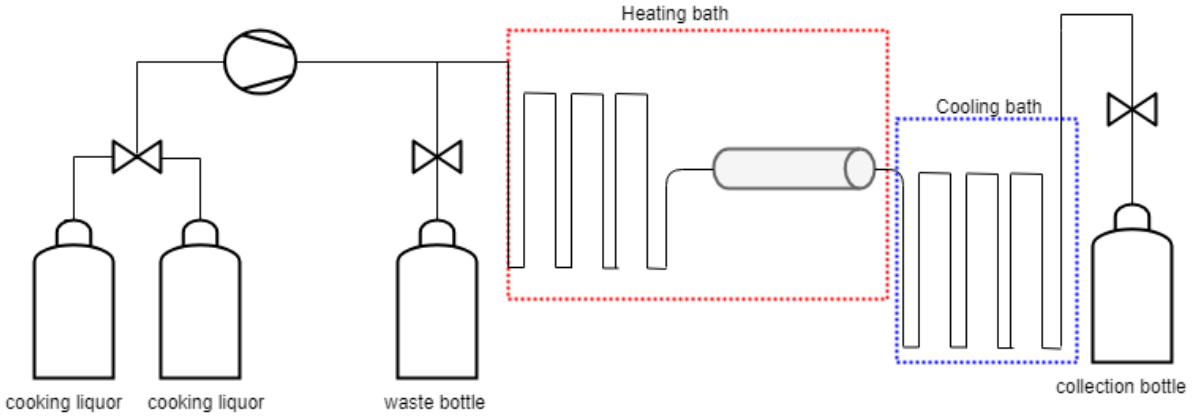

Figure 3.2: Schematic flow sheet of the experimental set up using small flow-through reactor

Figure 3.3: Experimental set up using small flow-through reactor

To ensure an even flow, the column was carefully packed with approximately 4 g of wood meal (dry weight). During the entire cooking, cooking liquor was continuously pumped through the reactor. The column was first impregnated with 3-4 free volumes of cooking liquor. To avoid overpressure, the flow rate was changed step wise. During the first two minutes of impregnation, the flow rate was set to 2.5 ml, followed by 5 ml/min after 3 minutes, 8 ml/min after 4 minute and finally 10 ml/min after 5 minutes of impregnation.

After the impregnation, the column was submerged into a hot oil bath of PEG at 115°C, and the set temperature of the bath was set to the desired end temperature (148, 158 or 168°C).

The flow rate was changed during the cooking according to Table 3.1. During the first 12 minutes of cooking, the flow rate was set to 10 ml/min. Between 12-22 minutes, the flow rate was 8 ml/min, and finally 2.5 ml/min during the remaining cooking time. After the predetermined cooking time, the column was placed in a cooling bath for 10 minutes and the flow rate was changed to 1 ml/min.

Table 3.1: The flow rate was changed during the impregnation, cooking and cool down. The left side of the backslash indicates the time for a cooking time of 180 minutes, and the right side that of a cooking time of 90 minutes

Time interval [min]	*Flow rate [ml/min]*	
0-2	2.5	Impregnation cycle
2-3	5	
3-4	8	
4-5	10	
0-12	10	Cooking
12-22	8	
22-180/90	2.5	
180/90-190/100	1	Cool down

Samples of black liquor (BL) were taken at given times during the cooking. The sample sequence and the respective volumes are seen in Table 3.2. Since the samples were cooled immediately, it was assumed that no more reactions were taking place after sampling. In total 8 BL samples were collected when the total cooking time was 180 minutes and 5 if the cooking time was 90 minutes.

Table 3.2: Sampling sequence of BL during the cooking

Sample	*Time interval [min]*	*Sample volume [ml]*
1	0-10	100
2	10-20	84
3	20-40	61
4	40-60	50
5	60-90 (+10 min for 90 min.)	75 (+10 for 90 min.)
6	90-120	75
7	120-150	75
8	150-180 (+10 min for 180 min.)	75(+10 for 180 min.)

The experimental series are seen in Table 3.3. The parameter of interest is the temperature and three different temperatures (148, 158 and 168°C) were evaluated. The temperature profiles of the three temperatures are seen in Figure 3.4.

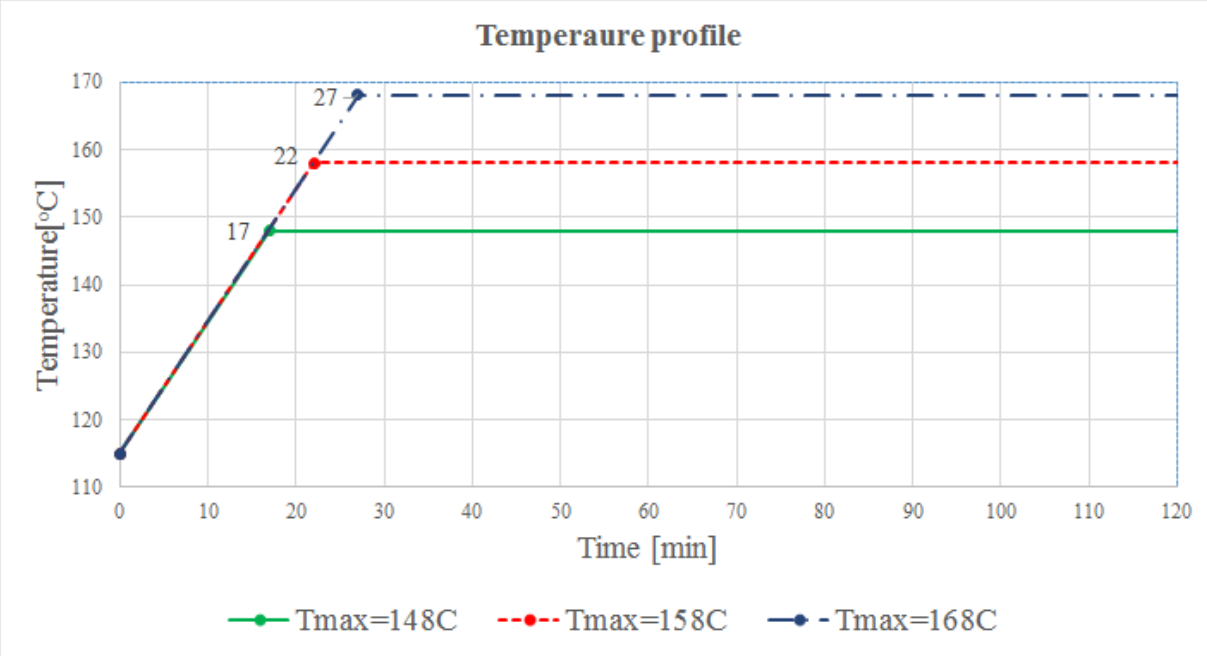

Figure 3.4: Temperature profile for the three maximal cooking temperatures. The labels in the graph indicate the time [min] needed to reach the desired temperature

To reach a temperature of 148°C, a heating up period of 17 minutes was required. For maximum temperatures of 158 and 168°C 22 and 27 minutes were needed respectively.

For each temperature and wood, two different cooking times were evaluated: 90 and 180 minutes. The experiments were performed randomized to avoid influence of nuisance factor.

Table 3.3: Experimental series

Wood meal	**T_{max} [°C]**	**Cooking time [min]**
Saw mill chips	148	90/180
	158	90/180
	168	90/180
Thinning material	148	90/180
	158	90/180
	168	90/180

The reason why these temperatures were chosen is because of good reference material from Dang (2017). Two cooking times were evaluated to get repeated points and also to get knowledge of the composition of the pulp at more than one time, thus to make more accurate mass balances.

3.4.1 The wood residue

The wood residue in the column was suspended in deionized water, filtered and dried at 105°C overnight, and saved for further analysis.

3.4.2 The black liquor samples

The black liquor samples were also saved for further analysis. 10 ml of each sample was saved for Klason analysis, 15 ml was saved as back-up and the remaining part was used for precipitation of lignin.

A method mentioned by Dang (2017) was used to isolate the lignin by acid precipitation. Drops of 95-97% sulphuric acid were added to the black liquior samples until the pH reached 2.5. The samples were let to rest in room temperature for 2 h. The samples were then placed in freezer at -18°C over night. The following day, the samples were thawed in room temperature and filtered. During the filtration, the samples were washed with acidic water at pH 2.5. The filters with the precipitated lignin were dried at 40°C for 2-3 days. The filters were then placed in a desiccator for 30 minutes before weighing. The precipitated lignin was scraped off and saved for GPC.

3.5 Analysis

Analysis was performed on the dried wood residue and the black liquor samples. The wood residue was analyzed for yield, Klason lignin, ASL and carbohydrate content. Analyzes of the BL samples included analysis of Klason lignin, ASL, MWD of the precipitated lignin and carbohydrate content. Analysis of Klason lignin, ASL and carbohydrate was also done three times on the untreated wood meal. This was done to gain information about the original composition of the wood and to get an estimation of the experimental error. The experimental error of the wood meal measurements ([% on wood]) of KL was estimated to ±2% and carbohydrate content ±0.5% on wood. Some analytical measurements were repeated, thus the experimental error could be estimated for these as well. For BL analysis, the experimental error ([% on wood]) of KL was estimated±0.09% and ASL ±0.02% using pooled standard deviations.

3.5.1 Klason lignin

Acid hydrolysis was performed according to the method described by Dang (2017). To the 10 ml fractions of BL, 72% H_2SO_4 was added until pH reach 1-1.5. The samples were then left to stand for 30 minutes and then warmed in a water bath at 30°C for 1 h. 8.93 ml of deionized water was added, followed by hydrolysis in autoclave at 125°C for 1 h. The samples were filtrated through a glass microfiber filter with warm deionized water into volumetric flasks containing 4 ml of fucose (200 mg/L), internal standard, to a total volume of 100 ml. The solid residues remaining after filtration were dried in oven at 105°C over night and determined gravimetrically.

As for the wood residues and the untreated wood meal, 250 g of wood meal/pulp was dried in the oven at 105°C over night. The pulp was disintegrated using *Yellow line A 10* grinder, to be easier to impregnate with H_2SO_4 in a later stage. To 200 mg of dry

material, 3 ml of 72% H_2SO_4 was added. The samples were then kept under vacuum for 15 minutes, followed by heating in a water bath at 30°C for 1 h. 84 g of deionized water was added and hydrolysis in autoclave at 125°C for 1 h followed. The samples were filtrated through a glass microfiber filter with warm deionized water when they were approximately 90°C. The solid residues remaining after filtration were dried in oven at 105°C over night and determined gravimetrically.

3.5.2 ASL measurement by UV

The filtrate obtained from the acid hydrolysis was diluted to 1/10 and 1/50 using fucose as internal standard. By measuring the absorbance at 205 nm with UV (*Specord 205 from AnalytikJena*), the amount of ASL in the original filtrate and the dilutions was quantified using Lambert Beer's law (Equation 2.2) assuming an absorptivity constant of 110 L $g^{-1}cm^{-1}$ (Lin & Dence 1992). Analysis of the data was done using *WinASPECT Software Vers. 2.3.10*.

3.5.3 Carbohydrate measurement by HPAEC-PAD

The original filtrates and the 1/10 and 1/50 dilutions obtained from the acid hydrolysis were freezed prior to analysis to avoid degradation of the carbohydrates. The filtrates were thawed and analyzed by HPAEC-PAD using *Dionex ICS-5000 HPIC* System equipped with a *Carbopac™PA1 column* and a guard column. The monomers arabinose, galactose, glucose, mannose and xylose were detected by a gold electrode in the detector. NaOH and NaAc+NaOH were the eluents used. The eluents were stored under helium.

Analysis of the data was done by *Chromeleon®, Chromatography Data System software, Dionex Chromeleon, Vers. 7.1.3.2425*. Using the detected amount of monomers the amount of anhydrosugars was calculated using the correction factor for the monomers (Janson (1974)) and the hydrolysis yield (Wojtasz-Mucha et al. (2017)), see Table 3.4.

Table 3.4: The correction factor and hydrolysis yield for the monomers detected

Monomer	Correction factor for monomers	Hydrolysis yield [%]
Arabinose	0.88	93.1 ± 1.9
Galactose	0.90	92.9 ± 1.7
Glucose	0.90	91.8 ± 2.0
Xylose	0.88	78.6 ± 1.6
Mannose	0.90	90.2 ± 0.6

3.5.4 Molecular weight of lignin by GPC

The MWD and M_w of the precipitated lignin was determined by GPC using the GPC system *PL-GPC Plus Integrated Instrument system*, equipped with both RI and UV (280 nm). 10 mg of the precipitated lignin was dissolved in 1 ml DMSO. 100 µL of the dissolved precipitates was added to 4 ml DMSO. From this solution, approximately 3 ml was filtered through a 0.2 µm filter on a syringe into a glass vial. Two injections were made for each sample and an average value was used.

DMSO with 10 mM LiBr was used as eluent. The separation took place at 50°C and at a flow rate of 0,5 ml/min. Calibration was done using 10 pullulan polysaccharide standards with MW: 0.180, 0.667, 5.9, 11.1, 21.1, 47.1, 107, 200, 375 and 708 kDa. Analysis of the data was done using software *Cirrus GPC Vers. 3.2*.

4
Results

The following chapter will display an interpretation of the results obtained from the cookings in the flow through reactor and analysis, accompanied by discussion. The results will be compared with the findings of Dang (2017). The comparability is high, since the studies of Dang (2017) also involves softwood. In parts of the studies, the same cooking chemical composition and maximum temperature are used, making it even more suitable for comparison.

Abbreviations used during this section are:

THN = Thinning material
SGV = Sawmill chips
90/180 = 90/180 minutes of cooking
L = T_{max}:148°C
M = T_{max}:158°C
H = T_{max}:168°C

Thus, the series name THN90L refers to an experiment where thinning material was used, a cooking time of 90 minutes and T_{max}:148°C

4.1 Cell wall thickness

The cell wall thickness was studied to investigate if there really was a difference in the cell wall thickness between the wood chips used. This was done using CLSM and the data was analyzed using the software *Fiji ImageJ*.

As can be seen in Figure 4.1, there is a broad range in the cell wall thickness. The distributions of the cell wall thickness of the thinning material and sawmill chips are seen in Figure B.1 and B.2 in *Appendix B*. The average cell wall thickness of the thinning material is 5.71 µm, while that of the sawmill chips is 6.83 µm. In literature, the cell wall thickness of spruce is reported to be 2-4 µm for earlywood and 4-8 µm for latewood (Sjöström 1993). Thus the obtained values fall within the region of latewood tracheids. As can be seen in Figure 4.1, the latewood tracheids appear more clear than the earlywood tracheids, and hence they were the ones measured. To get more knowledge about the cell wall thickness distribution, the earlywood tracheids should be measured as well. However, the purpose of this measurement was to evaluate whether the sawmill chips were the thicker ones, and on the respect of the latewood tracheids, they are.

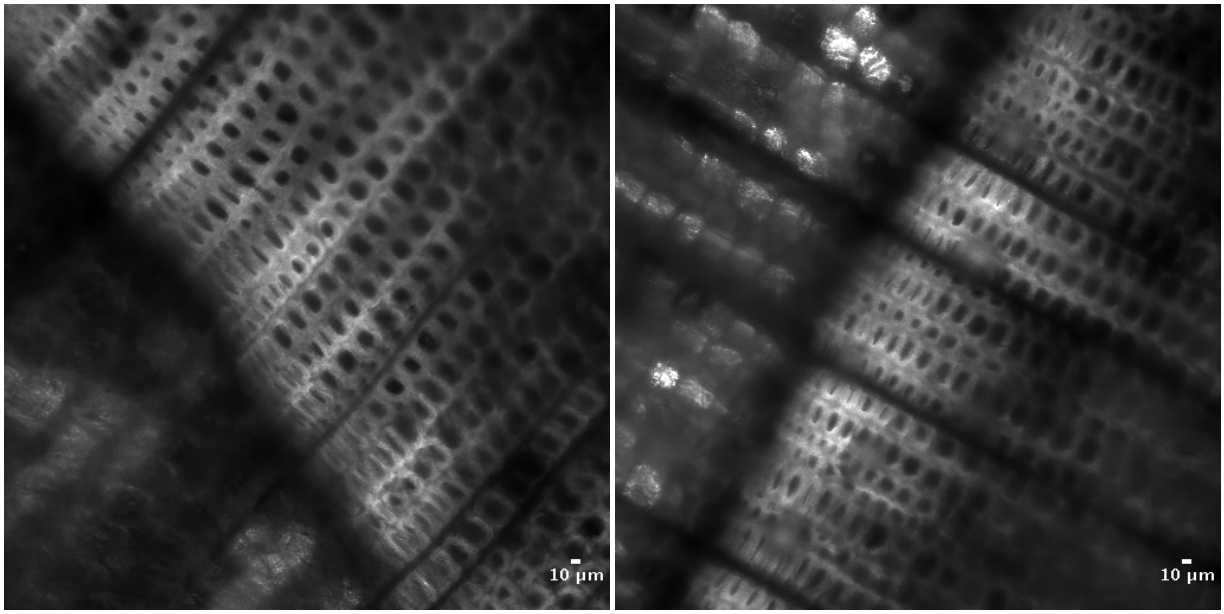

(a) Sawmill chips of spruce *(b) Thinning material of spruce*

Figure 4.1: CLSM-image of the cell wall structure of sawmill chips and thinning material of spruce. The black center is the lumen

Difficulties arose when cutting the wood chips into pieces that were thin and even enough to analyze. The reason why may be the wood chips being too dry. Preferably the chips should be cut when they are fresh and not after drying, which was the case here. This resulted in some damaged fibres and cracks in the cell wall, which made analysis difficult. The black lines in Figure 4.1 is probably the cracks that arose during cutting of the chips. Especially the thinning material was difficult to cut, which may be due to weaker cell walls.

The method of measuring the cell wall thickness can be further refined to get more clear images. In this analysis, no pretreatment of the wood was done, besides wet analyzing,

since the lignin is autoflourescent with maximum absorbance in the UV range. However, to reduce the background noise and enhance the contrast between cell wall and cell lumen, pretreatment with safranine has been reported to be useful (Liang et al. 2013). Safranine also generates different colors in the different cell wall layers, thus making it possible to label the layers of the cell wall (Bond et al. 2008).

4.2 Composition

The composition of the wood meal was obtained by analysis of the untreated wood meal, see Figure 4.2. The amount of cellulose, glucomannan and xylan was calculated according to *Appendix C*. It is concluded that cellulose constitutes the majority of the wood, followed by lignin. It is only Klason lignin that is included, and not the acid soluble lignin since it is not definite what it contains. "Other material" refers to material not being characterized, i.e ash, extractives, other polysaccharides, rhamnose, acids, acetyl groups and unidentified matter.

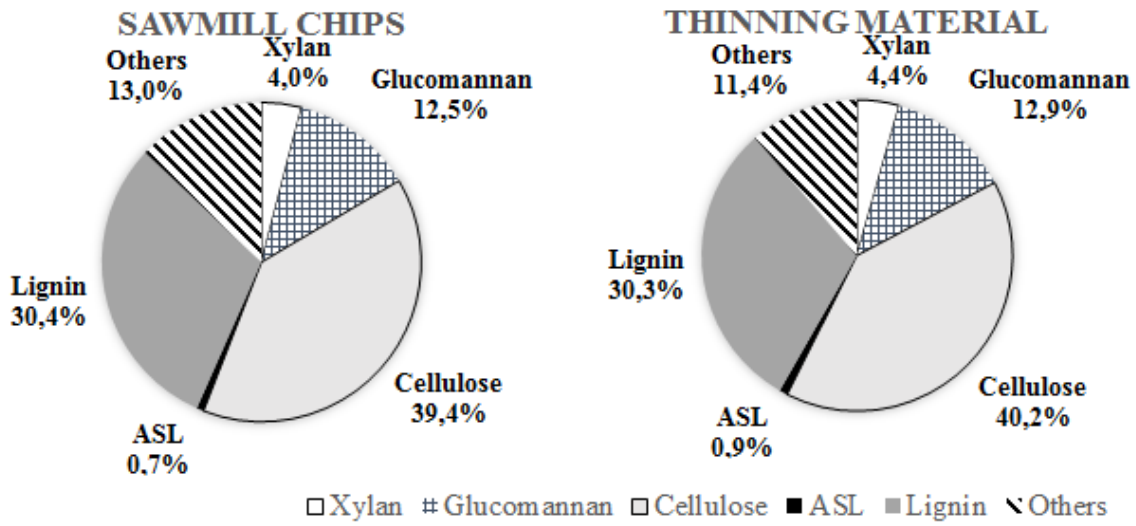

Figure 4.2: Composition of wood meal of sawmill chips and thinning material

Table 4.1: Comparison between literature values and experimental values. All values are given as % of dry wood weight

	Literature data (Sjöström 1993)	*Sawmill chips*	*Thinning material*
Total extractives	1.7	-	-
Lignin	27.4	30.4	30.3
Cellulose	41.7	39.4	40.2
Glucomannan	16.3	12.5	12.9
Xylan	8.6	4.0	4.4
Other polysaccharides	3.4	-	-
Residual constituents	0.9	-	-

Compared to the literature data found in Table 4.1, the values differ to some extent. The lower value of xylan might partly be explained by not including the acids, expressed in

parenthesis in Equation C.3. The obtained experimental values of lignin are somewhat higher than the literature value. A possible reason for the higher lignin value might be because the extractives were not removed prior to analysis, i.e some extractives may have condensed on the lignin structure. However, the difference may also be due to different choices of characterization methods.

4.3 Cooking experiments

The cooking experiments were conducted according to the method described in *3.4 Flow-through reactor*. Three maximum temperatures were evaluated; 148, 158 and 168 °C. The temperature profiles of the three temperatures are seen in Figure 3.4.

Figure 4.3 displays the BL fractions that were collected during the cooking according to Table 3.2. The colour of the BL fractions collected varied with time and temperature. The green colour of the last BL fraction shown in Figure 4.3 is found for a cooking temperature of 168 °C using both thinning material and sawmill chips. No analysis was done in order to find the reason behind why the sample turned green.

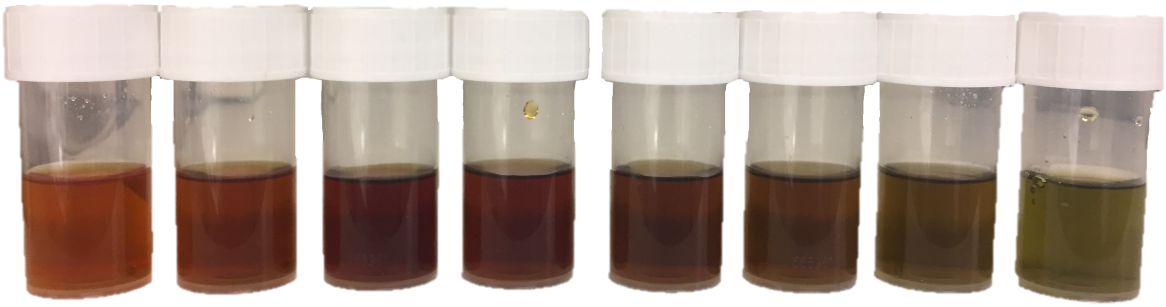

Figure 4.3: From the left: BL Fraction 1 - 8. The fractions collected are from thinning material, T_{max}:168 °C

4.3.1 Molecular weight

The following section will present the results from the GPC in section *3.5.4 Molecular weight of lignin by GPC*. It was only the precipitated lignin from the BL fractions that was analyzed using this method.

The average molecular weights in kDa for the three temperatures are shown in Figure 4.4-4.6. It can be noticed that a higher temperature results in a higher maximum molecular weight. This may be a result of condensation reactions, causing lignin entities to form larger complexes and/or that the mobility of lignin fragments increases with increasing temperature.

For a cooking temperature of 148°C, it is noticed that the Mw is increasing with time for the sawmill chips, whereas the thinning material shows a decrease at the last fraction (Figure 4.4). The lignin fragments follow the same molecular weight until the 6th fraction (120 minutes of cooking). In this sample and the following, a higher molecular weight fragment of lignin is found in the BL sample from the thinning material. In the last fraction (180 minutes of cooking), the larger lignin fragment is found in the BL fraction obtained from the sawmill chips. This could indicate that it takes longer time for large fragments to diffuse through the thicker cell wall. The theory proposed by Gellerstedt et al. (2004) that the delignification is retarded because of condensation reactions could be supported by these findings, since larger fragments require more time to diffuse through the cell wall.

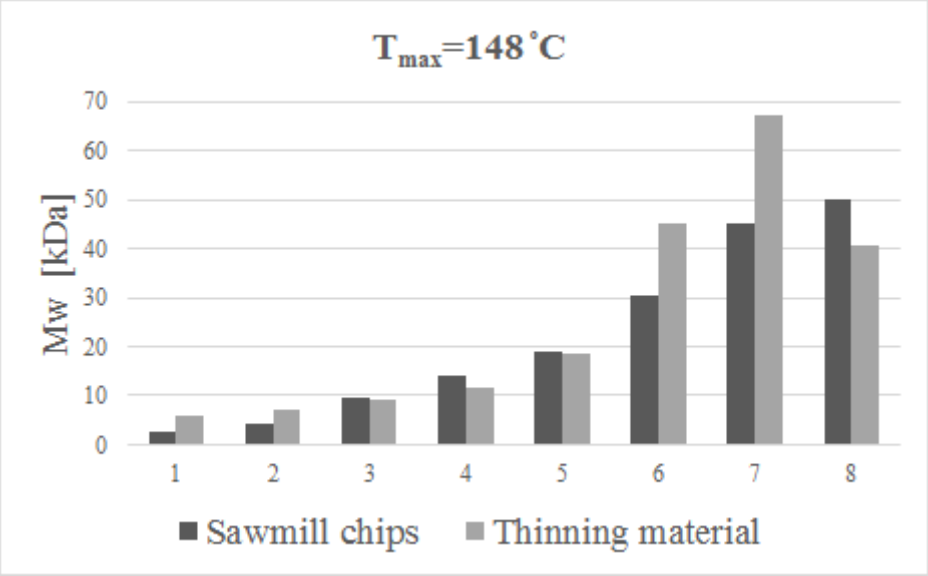

Figure 4.4: Average Mw of lignin, T_{max}:148°C

When the maximal cooking temperature is increased to 158 °C, the difference between the two wood meals can be noticed already in sample 5 (90 minutes of cooking), see Figure 4.5. The higher Mw is once again found in the BL fraction obtained from the thinning material. The maximum Mw of the thinning material is found in sample 6, while it is found in sample 7 for the sawmill chips. In similarity with the findings at 148 °C, this could indicate that the larger lignin fragments more easily diffuse through the thinner cell wall.

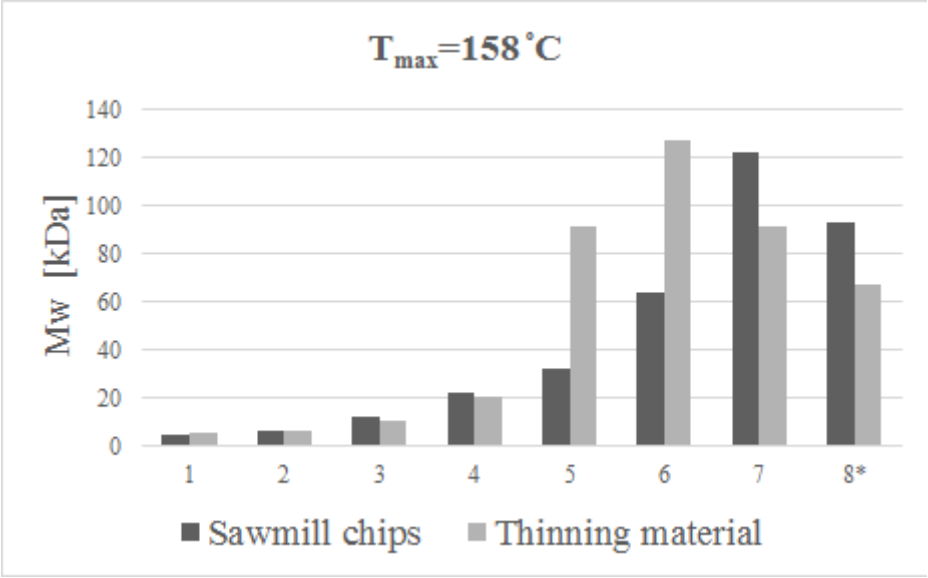

*Figure 4.5: Average Mw of lignin, T_{max}:158°C. * indicates questionable result*

At a cooking temperature of 168°C, the Mw of the thinning material reaches its maximum in sample 5, after which it descends (Figure 4.6). The PL from the sawmill chips follow the same trend, but the maximal Mw is drastically lower. The high peak in sample 5 for thinning material may be the result of analytic errors, or as mentioned, the result of condensation reactions. Samples with a small amount of PL were difficult to scrape off the filter. This was the case for sample 7 in thinning material 168°C and sample 7 and 8 in sawmill chips 168 °C. The solution was to add DMSO directly to the filter (10 mg PL/1 ml DMSO) and let it drip through during the day. The consequence of this may have been that only the small lignin fractions present were dissolved, thus the molecular weight may in fact have been larger than what is shown. The results obtained from the PL from BL fractions collected at longer cooking times could therefore be questioned. These samples are marked with * in Figure 4.6.

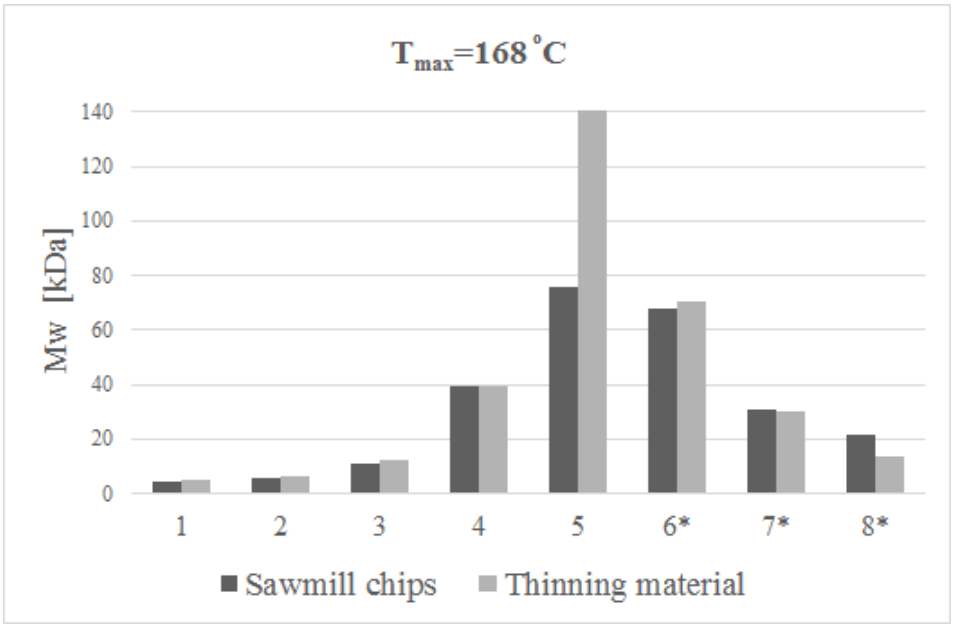

*Figure 4.6: Average Mw of lignin, T_{max}:168°C. * indicates questionable result*

The molecular weight distributions for each series are found in *Appendix D*. When comparing the MWD profiles with the ones obtained by Dang, Brelid & Theliander (2016), a similar shift towards a higher molecular weight size range is visible only at 148 °C. The MWD is wide for all samples, but the trend is that the fraction of low Mw fragments decreases with time. However, the last PL samples at 168 °C (see Figure D.11 and D.6), have much more narrow size distribution. This may be because not much lignin is left in the sample, since delignification might have been completed.

When comparing the Mw results with the findings of Dang, Brelid & Theliander (2016) for 158 °C, it is clear to see that they differ in some aspects. The maximum Mw is slightly higher (130 kDa) compared to the one obtained by Dang, Brelid & Theliander (2016) (90 kDa). Moreover, in the study performed by Dang, Brelid & Theliander (2016), the Mw increased over time, whereas the results obtained in this work indicates that Mw increase until a maximum occurs. The reason for this is not fully understood, but a possibility for the decreasing Mw may be that the lignin fragments were not completely dissolved, i.e only the smaller lignin fragments had been dissolved. Another possibility is that there was not much lignin left in the BL fraction, since the delignification was almost completed at the time of sampling. The acid precipitated lignin could therefore in these samples lack lignin.

4.3.2 Klason lignin

To study the effect on the delignification, the amount of klason lignin in the pulp as a function of time was investigated, see Figure 4.7. To determine the content of klason lignin in the pulp at various times, it is a possibility to perform several experiments with different cooking time. In this study, two cooking times (90 and 180 min) were performed. Thus to determine the content of KL in the pulp at various times, backward and forward balances were used, see *Appendix E*. Since there are duplicates for data points up to 90 minutes, average values are taken for these points. All series but SGV180H is performed only once. SGV180H is performed twice, thus an average value is presented. Since the result of the replicates differed to some extent, it would have been beneficial to perform an additional run to establish the result.

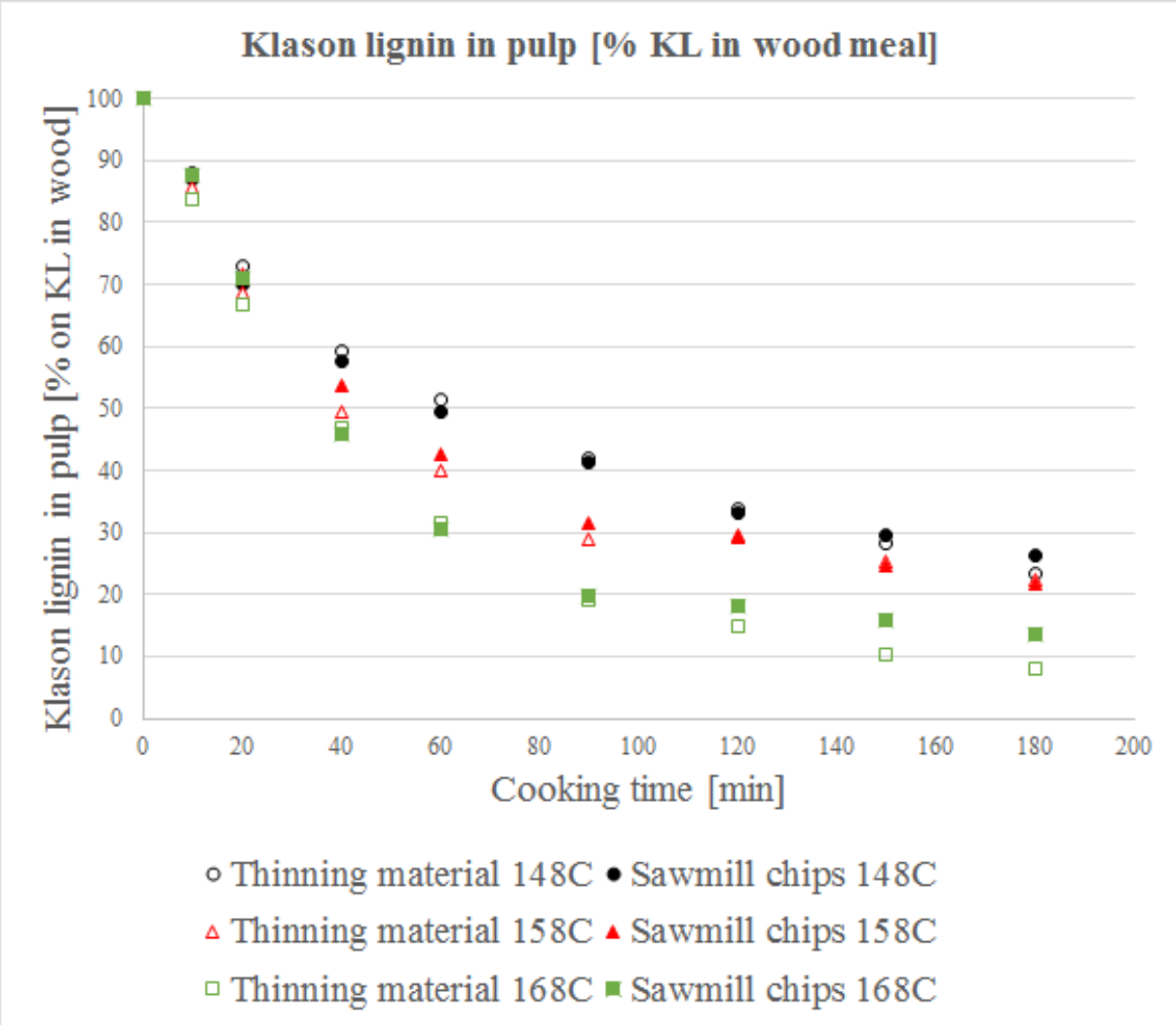

Figure 4.7: KL in pulp [% on KL in wood] as a function of time and temperature

During the heat up period, i.e approximately the first 20 minutes, the delignification follows similar pattern in all the experiments, as was expected since the same conditions prevailed. After the initial heating up period, an increased maximum temperature results in faster delignification. The delignification is fast until 90 minutes, after which it slows down for all temperatures. The retardation of the delignification rate may be due to

condensation reaction, as suggested by Gellerstedt et al. (2004) and indicated in Figure 4.4-4.6. However, it may also be because the smaller lignin fragments already have been removed, hence larger fragments remain in the wood matrix and these require longer time to diffuse through the cell wall.

The delignification of sawmill chips and thinning material follow the same trend for 148 and 158 °C, i.e it does not seem to depend on the difference in cell wall thickness. However, at 168 °C, a difference is noticed after 120 minutes. After 120 minutes, the resulting lignin fragments formed or originally in the wood matrix, may have reached a critical size, where the difference in diffusion rate becomes significant. Larger lignin fragments need longer time to diffuse through the thicker cell wall of the sawmill chips compared to that through the thinner walls of the thinning material, as indicated by the findings in Figure 4.4-4.6. In other words, the increased Mw of the lignin fragments (native lignin, or caused by condensation reactions) might have resulted in different diffusion rates through the cell wall. This has in turn lead to different delignification kinetics.

4.3.3 Sugar analysis

The sugar content of the pulp, black liquor and wood meal was determined, and the results are presented in the following section.

Figure 4.8 displays all the anhydrosugars detected in the pulp, expressed as relative amounts of the anhydrosugars in the wood meal. Analyzing the concentration of the anhydrosugars of the pulp showed that glucose was not as affected by temperature or time, as was expected. A major reason for the trend observed is due to cellulose being quite resistant towards degradation/dissolution during the cooking.

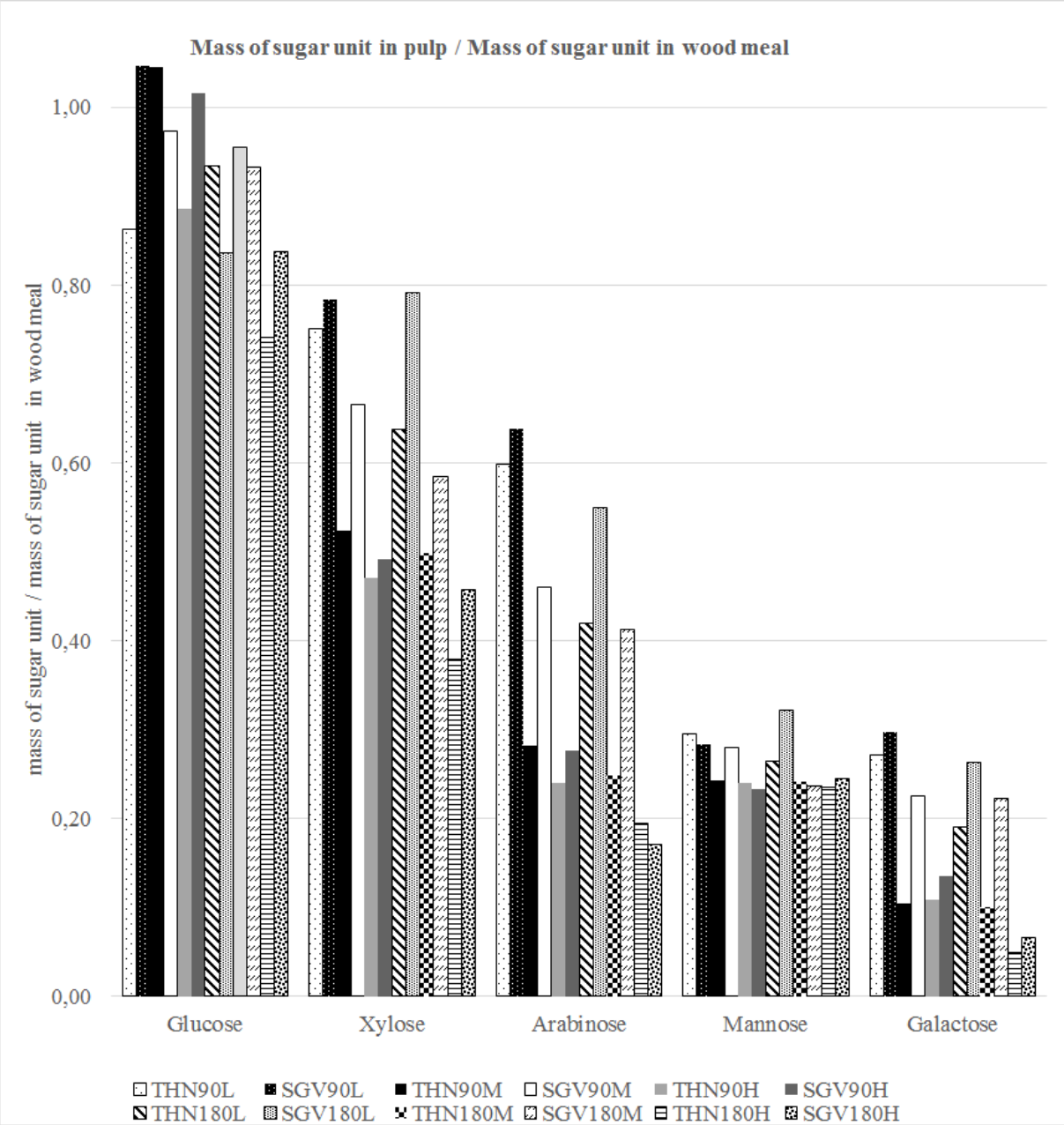

Figure 4.8: The relative amounts of anhydrosugars detected in the pulp for each series

It is noticed in Figure 4.8 that pulp THN90L has a low amount of glucose, which might be due to shortcomings with the analysis. On the other hand, pulp from series SGV90L,

THN90M and SGV90H have more glucose in the pulp than in the wood meal. Moreover, these deviations are within the experimental errors. Conclusions to be taken regarding the glucose in the pulp is that it is the least affected sugar.

However, the major building blocks of the hemicelluloses (mannose, galactose, arabinose and xylose), were affected to a some extent, see Figure 4.9, where they are presented separately.

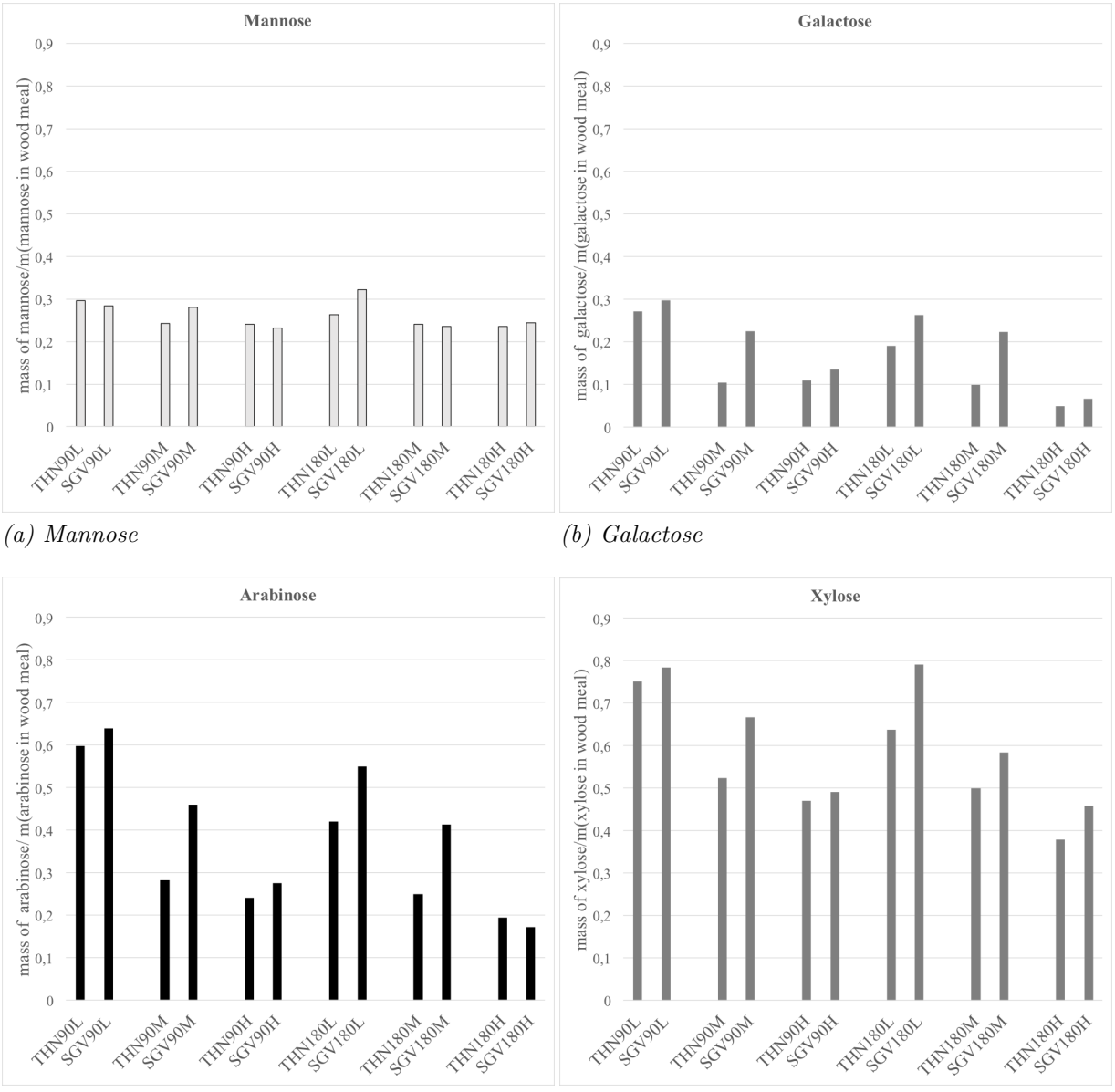

(a) Mannose

(b) Galactose

(c) Arabinose

(d) Xylose

Figure 4.9: Anhydrosugars detected in the pulp, expressed as relative amounts of the anyhdrosugars in the wood meal.

The amount of mannose seems to be independent of temperature, time and cell wall thickness, see Figure 4.9 A. This would indicate that the the degradation and dissolution of (galacto)glucomannans is very rapid. This agrees well with what has been previously reported (Sjöström (1993), Wigell et al. (2007), Aurell (1965)).

Unlike the behaviour of mannose, the degradation/dissolution of arabinose (Figure 4.9 C) seems to be dependent upon temperature and time, and also cell wall thickness to some extent. Higher values of arabinose are noticed in all sawmill pulps, except for the one at 180 minutes and 168°C (SGV180H). Arabinose is the sidegroup of xylan, which has been suggested to have close connection with the lignin (Wigell et al. 2007). Therefore, it is not surprising that xylose and arabinose follow the same trend. The reason why there is no influence of the cell wall thickness after 180 minutes of cooking at 168°C may be because after longer time and higher temperatures, most of the arabinose have been peeled off the xylan backbone.

Another trend noticed in Figure 4.9 is that galactose and xylose follow the same trend, i.e that higher amounts of the anhydrosugars are detected in the sawmill pulps. In similarities with the arabinose, the amount detected in the pulp is decreasing with temperature and time. A comparison between mannose (Figure 4.9 A) and galactose (Figure 4.9 B) show that they do not follow the same trend, even though they both are building blocks in the (galacto)glucomannans. The behaviour of the (galacto)glucomannans in spruce during alkaline pulping has been studied e.g by Berglund et al. (2019). They suggest that the different behaviour is because of a higher stability of the galactose, which prevent them from being degraded to the same extent as mannose. Moreover, this does not explain the similar behaviour of xylose, galactose and lignin, i.e that they are consistently found in greater amounts in the pulp of sawmill chips. The reason behind this phenomena is not fully understood.

Xylose, galactose and arabinose, were the anhydrosugars detected in largest amounts in the BL, which agrees with previous studies (Dang et al. 2018). Xylose is reported in literature to be the predominant anhydrosugar found in Kraft BL (Niemelä 1999). The assumed origins of the monosugars detected in the BL fractions are seen in Figure 4.10.

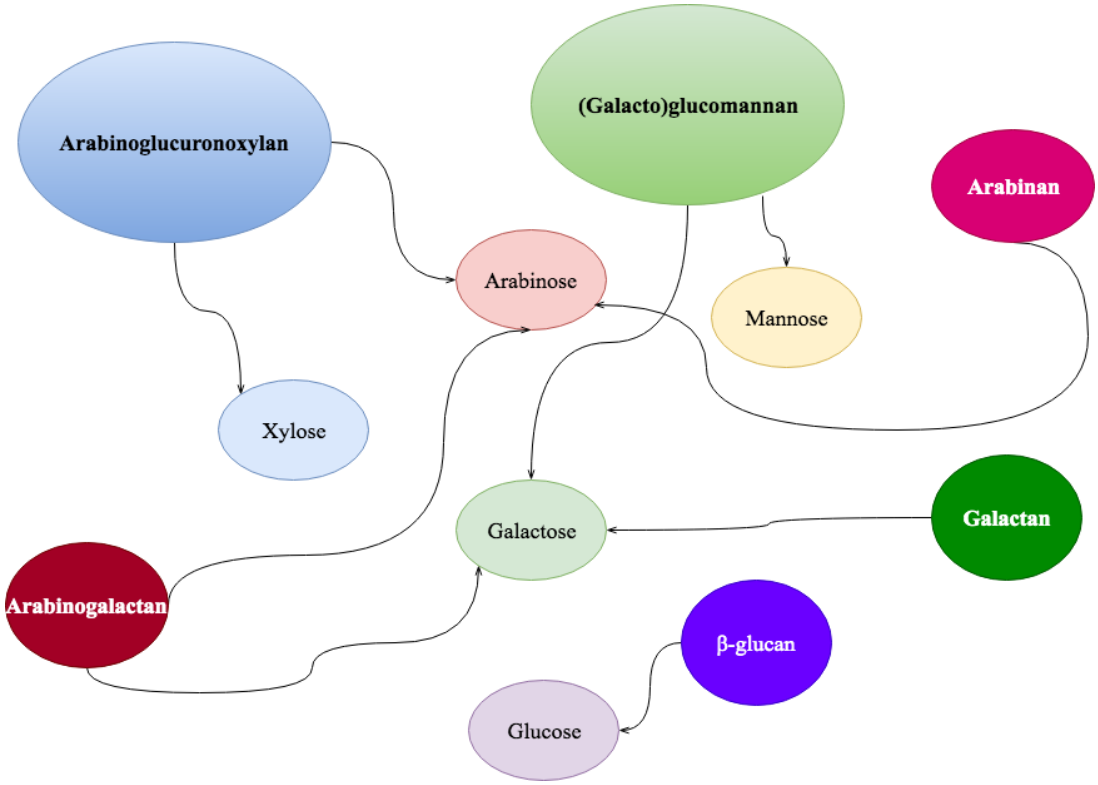

Figure 4.10: The assumed origin of the monosugars detected in the BL fractions, pulp and wood meal

The xylose detected was assumed to originate from the arabinonoglucoronoxylan and the mannose from the (galatacto)glucomannan. The arabinose does not only originate from the arabinoglucuronoxylan, but small amount may also originate from the arabinan and arabinogalactan. The galactose may originate from the (galacto)glucomannan, but also small amounts from the galactans and arabinogalactans. However, not all the monosugars in the filtrate derive from the anhydrosugars when analyzing black liquor. Some monosugars detected come from degradation of saccharinic acid galactoside residues created during pulping (Dang et al. 2018). Since the BL fractions are quenched immediately after exiting the reactor, it is assumed that no further reactions take in the BL after sampling. Small amounts of glucose were detected at the longer cooking times at 168°C. Dang et al. (2018) also noticed this phenomena and suggested that the glucose fragments come from β-glucan. That glucose is only detected at high temperature may be due to the wood matrix being loosened enough for material to diffuse from the wood cell.

However, some of the monosugars are peeled off and end up as isosaccharinic acids or stable metasaccharinic acids in the black liquor. These acids cannot be quantified, which complicates the analysis of the BL sugars. An estimation of the monosugars ending up as acids in the BL fractions is achieved by material balances, see *Appendix F*. To determine in what period during the cooking the acids were formed, the amount of acids formed during 0-90 minutes and 90-180 minutes were calculated. The result is seen in Figure 4.11. THN L is missing due to low glucose values of the pulp for 90 minutes, which resulted in negative amount of acids being formed during the later part of the cook.

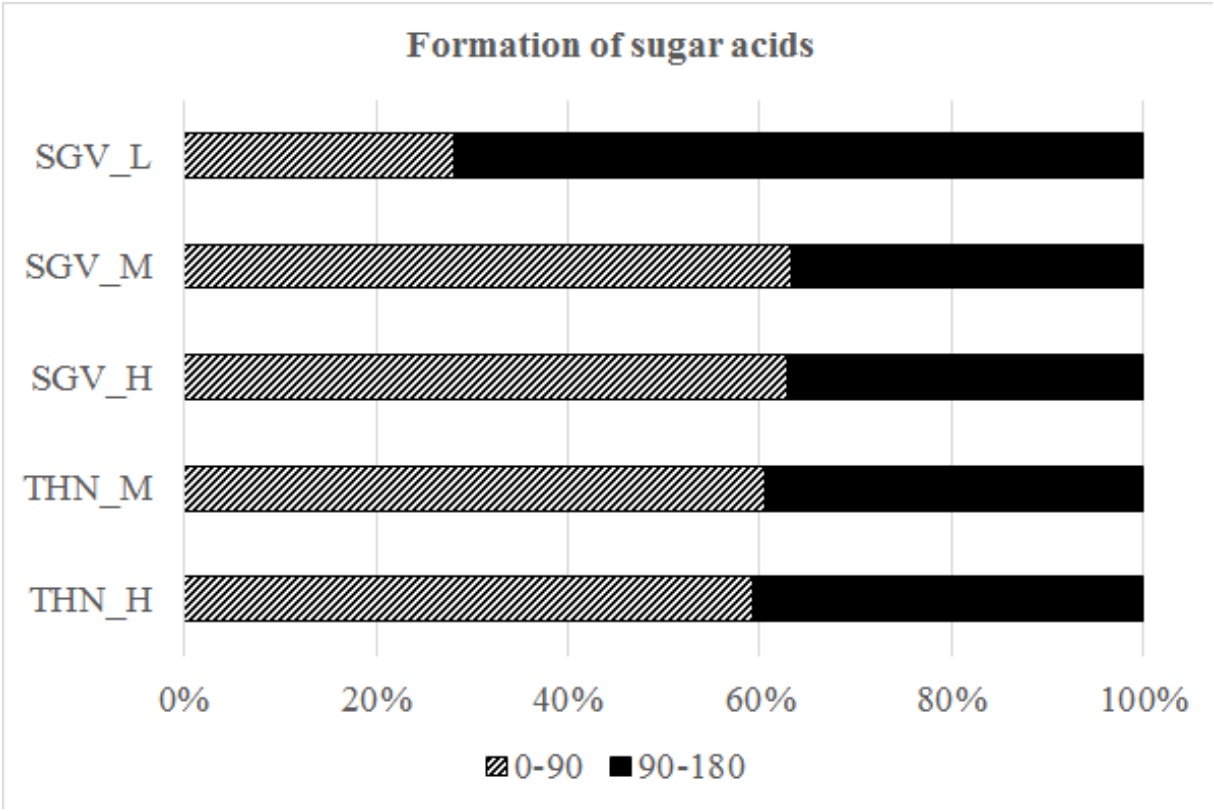

Figure 4.11: The amount of acids created during 0-90 and 90-180 minutes of cooking

The trend seen in Figure 4.11 is that more acids are formed during the first 90 minutes compared to the last, with the exception of sawmill chips 148°C. Since the degradation/dissolution of (galacto)glucomannan has been reported to be very fast during the initial part of the cook (Sjöström (1993), Wigell et al. (2007), Aurell (1965)) and since xylose is prevented against peeling, it agrees with the findings that more acids are formed during the first part of the cook. Regarding the result for 148°C it is difficult to establish the validity of this result, since there is only one replicate at this temperature.

Mannose, galactose and xylose were monosugars of special interest. Mannose, to study the peeling reaction of (galacto)glucomannan; xylose, to study the prevention of the peeling reaction, and galactose to study the phenomena noticed in Figure 4.9 B, i.e that more galactose remained in the pulp from the sawmill chips. Hence, the formation of isosaccharinic and alkali stable-metasaccharinic acids were calculated by subtracting the amount of sugar in the pulp+BL from the amount of sugar in the wood meal. The amounts of sugar acids from mannose, xylose and galactose are seen in Figure 4.12-4.14. Please note that the y-axis shows the mass of sugar/mass of sugar in wood meal.

There is a large difference between the amount of mannose in the wood meal and the amount found in the BL fractions and the pulp, see Figure 4.12.

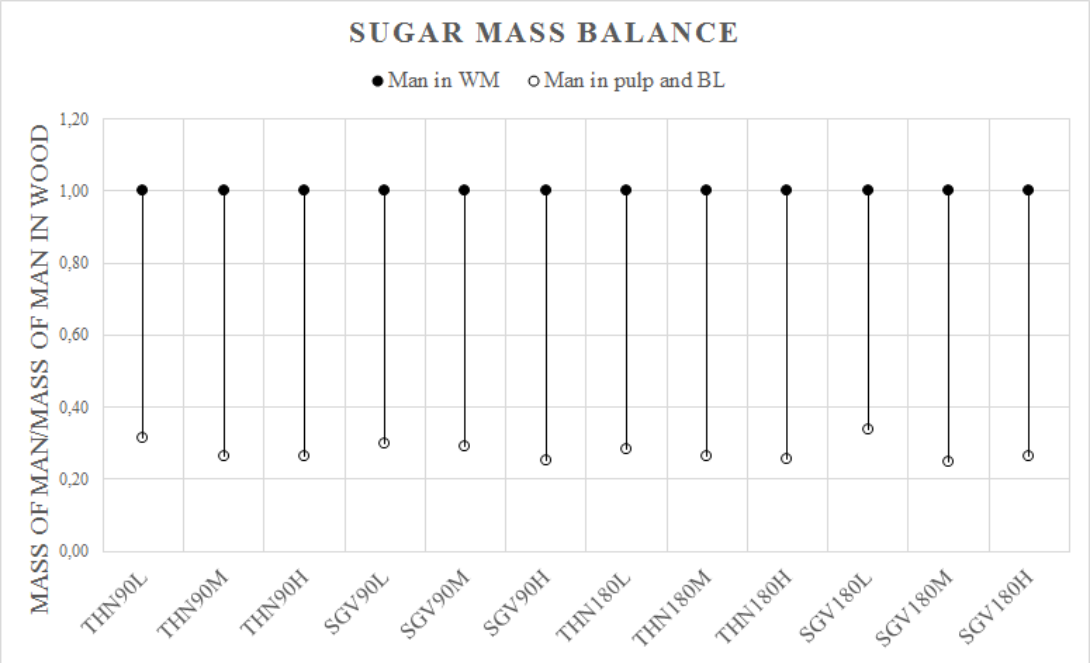

Figure 4.12: Mass balance of mannose

The reason behind the difference between the wood meal and the BL+pulp is a result of a lot of acids being formed. Once again, there is an indication that the (galacto)glucomannan reaction is rapid, since there is not much of a difference when comparing the acid being formed after 90 minutes compared to after 180 minutes, i.e the formation of acids seems to have ended after 90 minutes.

The mass balance of xylose in Figure 4.13 differs a lot from the one of mannose. Since the difference between amount of xylose in the wood meal and the amount found in BL+pulp is small, it is assumed that the amount of acids being formed is minor. These findings suggest that xylan is well shielded against peeling, in good agreement with Sjöström (1993) and Teleman (2009).

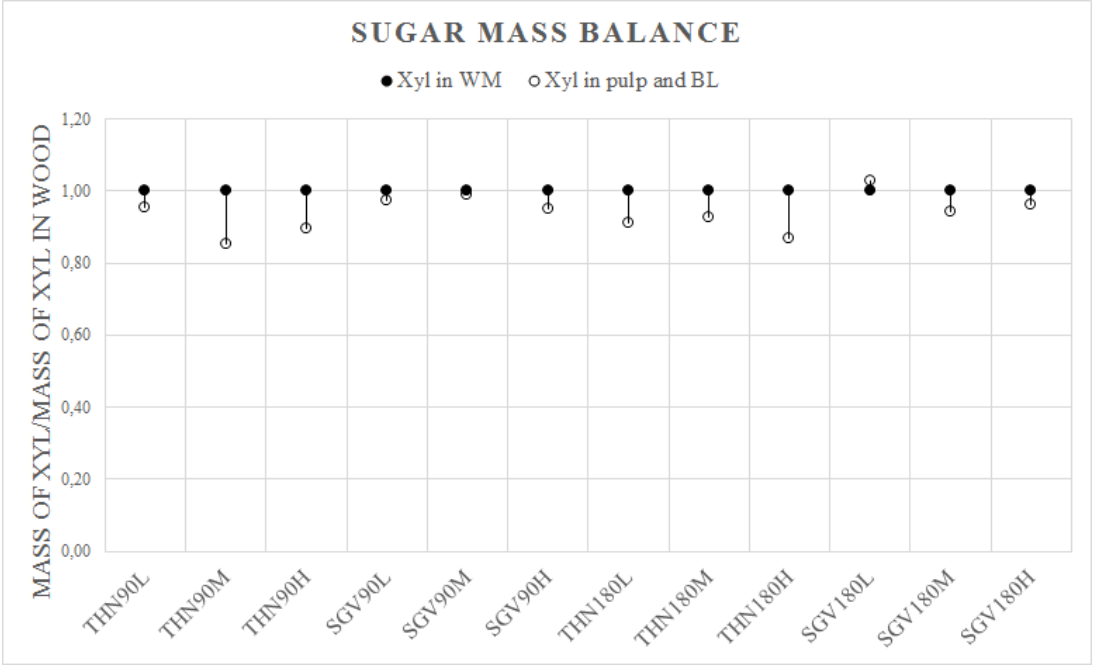

Figure 4.13: Mass balance of xylose

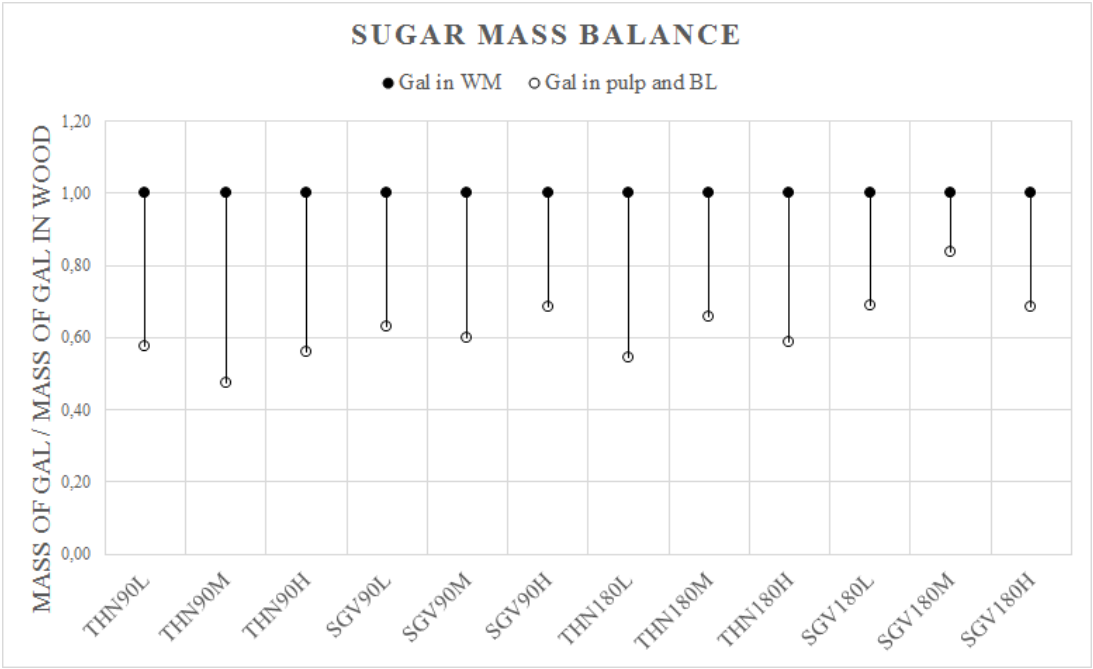

Figure 4.14: Mass balance of galactose

There is no clear trend found in Figure 4.14, the mass balance of galactose. However, compared to the mannose, less acids are being formed. Hence it might be an indication that the galactose is less prone to degrade, which supports the theory of a higher stability as described by Berglund et al. (2019).

5
Conclusion

The objective of this thesis was to establish the impact that the cell wall thickness has on the Kraft cooking kinetics. The conclusions obtained after performing experiments in a small flow-through reactor, quantification of lignin and carbohydrates in BL fractions and in pulp, and determination of MWD and Mw of lignin through several analytical techniques, are as follows:

- The results show that delignification is independent of cell wall thickness for temperatures under 168 °C and cooking times under 120 minutes for a constant ionic strength of $[Na^+]$=0.52 mol/kg solvent and constant $[OH^-]$ and $[HS^-]$ of 0.26 mol/kg solvent. After 120 minutes at a cooking temperature of 168°C, different delignification rates could be noticed. The delignification seemed to occur faster using thinning material. This may be a result of increased Mw of lignin, which impedes the delignification. However, replicates should be performed in order to establish the results.

- The maximum Mw of dissolved lignin increase with temperature, which may be a result of condensation reactions and/or higher mobility. This is another reason for keeping the cooking temperature as low as possible, besides increasing the yield and energy efficiency. The results also show that larger lignin fragments need longer time to diffuse through the cell walls of sawmill chips compared to thinning material.

- Xylose and galactose were consistently found in higher amounts in the pulp from saw mill chips. Xylose seemed to be protected against peeling reaction, resulting in minor amounts of acids being formed.

- Mannose is rapidly degradaded/dissolved under prevailed cooking conditions, and did not seem to be affected by an increment of the cell wall thickness.

To summarize; the findings in this Master's Thesis suggest that the cell wall thickness might have an impact on the kraft cooking kinetics, but more research is required to establish this.

6
Outlook

At the end of this project, some thoughts on how to improve the work arose. A future outlook is therefore presented in the list below.

- Removal of extractives prior to cooking to avoid disturbance of dissolved extractives
- Increase the cooking time, to see if a difference is noticed for 148 and 158°C at longer times
- Perform replicates for 168°C to establish findings
- Perform more and shorter cooks to track the carbohydrate reactions
- Include NMR to get knowledge of the lignin linkages
- Improvement of method used for determining cell wall thickness
- Investigate the influence of ionic strength. Dang (2017) noticed that the delignification rate was decreased with increased ionic strength and it would be interesting to see if the effect is more pronounced in sawmill chips

Bibliography

Aurell, R. (1965), 'Kraft pulping of pine. part 1', *Sven Papperstidn* **68**, 59–68.

Basu, P. (2018), *Biomass Gasification, Pyrolysis and Torrefaction - Practical Design and Theory*, 3rd edn, Elsevier.

Berglund, J., Azhar, S., Lawoko, M., Lindström, M., Vilaplana, F., Wohlert, J. & Henriksson, G. (2019), 'The structure of galactoglucomannan impacts the degradation under alkaline conditions', *Cellulose* **26**(3), 2155—2175.

Bhattacharya Sati, N., Kamal Musa, R. & Gupta Rahul, K. (2011), *Polymeric Nanocomposites - Theory and Practice*, Hanser Publishers.

Biermann, C. J. (2012*a*), *Handbook of Pulping and Papermaking . 5.3.6 Klason Lignin, Acid Insoluble Lignin*, Elsevier.

Biermann, C. J. (2012*b*), *Handbook of Pulping and Papermaking (2nd Edition)*, Elsevier.

Bogren, J. (2008), *Further insights into kraft cooking kinetics*, Chalmers University of Technology.

Bogren, J., Brelid, H., Karlsson, S. & Theliander, H. (2009), 'Can the delignification rate be affected by previously applied cooking conditions?.', *NORDIC PULP PAPER RESEARCH JOURNAL* **24**(1), 25 – 32.

Bond, J., Donaldson, L., Hill, S. & Hitchcock, K. (2008), 'Safranin fluorescent staining of wood cell walls', *Biotechnic histochemistry : official publication of the Biological Stain Commission* **83**, 161–71.

Brännvall, E. (2009), Chapter 6. pulping technology, *in* 'Pulp and paper chemistry and technology. [Volume 2]', Berlin : De Gruyter, c2009.

Brännvall, E. (2017), 'Peer-reviewed review article the limits of delignification in kraft cooking', *Bioresources* **12**, 2081–2107.

Chiang, V., Cho, H., Puumala, R., Eckert, R. & Fuller, W. (1987), 'Alkali consumption during kraft pulping of douglas-fir, western hemlock, and red alder.', *Tappi journal* .

Chiang, V. L., Yu, J. & Eckert, R. C. (1990), 'Isothermal reaction kinetics of kraft delignification of douglas-fir', *Journal of Wood Chemistry and Technology* **10**(3), 293–310.

Dang, B. T., Brelid, H. & Theliander, H. (2016), 'The impact of ionic strength on the molecular weight distribution (mwd) of lignin dissolved during softwood kraft cooking in a flow-through reactor.', *Holzforschung* (6), 495.

Dang, B. T., Brelid, H. & Theliander, H. (2018), 'Carbohydrate content of black liquor and precipitated lignin at different ionic strengths in flow-through kraft cooking.', *Holzforschung* (7), 539.

Dang, B. T. T. (2017), *On the Course of Kraft Cooking : the impact of ionic strength.*, Doktorsavhandling vid Chalmers tekniska högskola. Ny serie: 4306, Göteborg : Chalmers University of Technology, 2017.

Dang, B., Theliander, H. & Brelid, H. (2016), What do we know regarding the kinetics of delignification in kraft cooking?, *in* '4th European Workshop on Lignocellulosics and Pulp', Autrans, France.

Daniel, G. (2009), Chapter 3. wood and fibre morphology, *in* 'Pulp and paper chemistry and technology. [Volume 1]', Berlin : De Gruyter, c2009.

Deshpande, R., Henriksson, G., Germgård, U., Giummarella, N.and Lawoko, M., Sundvall, L. & Grundberg, H. (2018), 'The reactivity of lignin carbohydrate complex (lcc) during manufacture of dissolving sulfite pulp from softwood', *Industrial Crops and Products* **115**, 315 – 322.

Erickson, M., Larsson, S. & Miksche, G. E. (1973), 'Gaschromatographische analyse von ligninoxydationsprodukten. viii. zur struktur des lignins der fichte', *Acta Chem. Scand* **27**(3), 903–914.

Evstigneyev, Edward I.and Shevchenko, S. M. (2019), 'Structure, chemical reactivity and solubility of lignin: a fresh look', *Wood Science and Technology* **53**(1), 7–47.

Fengel, D. & Wegener, G. (2011), *Wood : chemistry, ultrastructure, reactions.*, Berlin ;Boston : De Gruyter.

Gellerstedt, G. (2009*a*), Chapter 5. chemistry of pulping, *in* 'Pulp and paper chemistry and technology. [Volume 2]', Berlin : De Gruyter, c2009.

Gellerstedt, G. (2009*b*), Chapter 9. analytical methods, *in* 'Pulp and paper chemistry and technology. [Volume 1]', Berlin : De Gruyter, c2009.

Gellerstedt, G., Majtnerova, A. & Zhang, L. (2004), 'Towards a new concept of lignin condensation in kraft pulping. initial results.', *Comptes rendus - Biologies* **327**(9), 817 – 826.

Gierer, J. (1980), 'Chemical aspects of kraft pulping', *Wood Science and Technology* **14**(4), 241–266.

Gierer, J. & Noren, I. (1980), 'On the course of delignification during kraft pulping.', *Holzforschung* **34**(6), 197–200.

Harada, H. & Côté, JR., W. (1985), 'Chapter 1: Structure of wood.', *Biosynthesis and biodegradation of wood components* pp. 1 – 42.

Henriksson, G. (2009*a*), Chapter 6. hemicelluloses and pectins, *in* 'Pulp and paper chemistry and technology. [Volume 1]', Berlin : De Gruyter, c2009.

Henriksson, G. Lennholm, H. (2009*b*), Chapter 4. cellulose and cabohydrate chemistry, *in* 'Pulp and paper chemistry and technology. [Volume 1]', Berlin : De Gruyter, c2009.

Henriksson, G., Lennholm, H. & Brännvall, E. (2009), Chapter 2. the trees, *in* 'Pulp and paper chemistry and technology. [Volume 1]', Berlin : De Gruyter, c2009.

Janson, J. (1974), 'Analytik der polysaccharide in holz und zellstoff', *Faserforschung und Textiltechnik* **25**, 375–382.

Lawoko, M., Henriksson, G. & Gellerstedt, G. (2003), 'New method for quantitative preparation of lignin-carbohydrate complex from unbleached softwood kraft pulp: Lignin-polysaccharide networks i.', *Holzforschung* **57**(1), 69–74.

Lawoko, M., Henriksson, G. & Gellerstedt, G. (2005), 'Structural differences between the lignin-carbohydrate complexes present in wood and in chemical pulps', *Biomacromolecules* **6**(6), 3467–3473.

Liang, W., Heinrich, I., Helle, G., Liñán, I. D. & Heinken, T. (2013), 'Applying clsm to increment core surfaces for histometric analyses: A novel advance in quantitative wood anatomy', *Dendrochronologia* **31**(2), 140 – 145.

Lin, S. Y. & Dence, C. W. (1992), *Methods in Lignin Chemistry. [electronic resource].*, Springer Series in Wood Science, Berlin, Heidelberg : Springer Berlin Heidelberg, 1992.

Lindgren, C. & Lindström, M. (1996), 'The kinetics of residual delignification and factors affecting the amount of residual lignin during kraft pulping', *Journal of Pulp and Paper Science* **22**(8), J290–J295.

Mattsson, C., Hasani, M., Theliander, H., Dang, B. & Mayzel, M. (2017), 'About structural changes of lignin during kraft cooking and the kinetics of delignification.', *Holzforschung* **71**(7-8), 545–553.

Mechelke, M., Herlet, J.and Schwarz, W., Zverlov, V. & Liebl, W.and Kornberger, P. B. J. (2017), 'Hpaec-pad for oligosaccharide analysis—novel insights into analyte sensitivity and response stability.', *Analytical and Bioanalytical Chemistry* **409**(30), 7169–7181.

Niemelä, K.and Alén, R. (1999), *Characterization of Pulping Liquors*, Springer Berlin Heidelberg, pp. 193–231.

Nieminen, K., Paananen, M. & Sixta, H. (2014), 'Kinetic model for carbohydrate degradation and dissolution during kraft pulping', *Industrial & Engineering Chemistry Research* **53**(28), 11292–11302.

Nishimura, H., Watanabe, T., Kamiya, A., Nagata, T. & Katahira, M. (2018), 'Direct evidence for ether linkage between lignin and carbohydrates in wood cell walls.', *Scientific Reports* **8**(1).

Olsson, C. & Westman, G. (2013), Direct dissolution of cellulose: Background, means and applications, *in* T. van de Ven & L. Godbout, eds, 'Cellulose', IntechOpen, Rijeka, chapter 6.
URL: *https://doi.org/10.5772/52144*

Plomion, C., Leprovost, G. & Stokes, A. (2001), 'Wood formation in trees', *Plant Physiology* **127**(4), 1513–1523.
URL: *http://www.plantphysiol.org/content/127/4/1513*

R. Obst, J. (1983), 'Kinetics of alkaline cleavage of -aryl ether bonds in lignin models: Significance to delignification', *Holzforschung* **37**, 23–28.

Rohrer, J. (2013), 'Analysis of carbohydrates by high-performance anion-exchange chromatography with pulsed amperometric detection (hpae-pad)', *Thermo Fisher Scientific* pp. 1–11.

Sjöström, E. (1993), *Wood Chemistry*, second edn, Academic Press, San Diego.

Skogsindustrierna (2018), 'Massa - produktion och handel'.
URL: *https://www.skogsindustrierna.se/skogsindustrin/branschstatistik/massa-produktion-och-handel/*

Sun, R.-C. (2010), *Cereal Straw as a Resource for Sustainable Biomaterials and Biofuels - Chemistry, Extractives, Lignins, Hemicelluloses and Cellulose*, Elsevier.

Teleman, A. (2009), Chapter 5. hemicelluloses and pectins, *in* 'Pulp and paper chemistry and technology. [Volume 1]', Berlin : De Gruyter, c2009.

Theander, O. & Westerlund, E. (1986), 'Studies on dietary fiber. 3. improved procedures for analysis of dietary fiber.', *Journal of Agricultural and Food Chemistry* **34**(2), 330–336.

Vroom, K. (1957), 'The h factor: A means of expressing cooking times and temperatures as a single variable', *Pulp Paper Mag. Can.* **58**(3), 228–231.

Wigell, A., Brelid, H. & Theliander, H. (2007), 'Degradation/dissolution of softwood hemicellulose during alkaline cooking at different temperatures and alkali concentrations.', *NORDIC PULP AND PAPER RESEARCH JOURNAL* (4), 488.

Willfor, S. & Holmbom, B. (2004), 'Isolation and characterisation of water soluble polysaccharides from norway spruce and scots pine.', *WOOD SCIENCE AND TECHNOLOGY* **38**(3), 173 – 179.

Wojtasz-Mucha, J., Hasani, M. & Theliander, H. (2017), 'Hydrothermal pretreatment of wood by mild steam explosion and hot water extraction', *Bioresource Technology* **241**, 120 – 126.

Yllner, S. & Enström, B. (1956), 'Studies of the adsorption of xylan on cellulose fibres during the sulphate cook. part 1', *Svensk papperstidning* **59**(6), 229.

A

Calculations ABC-titration

Sodium sulphide is dissolved in water and decomposed into sodium ions, hydroxide ions and hydrogen sulphide ions according to Equation A.1.

$$Na_2S + H_2O \rightarrow 2Na^+ + OH^- + HS^- \tag{A.1}$$

The current concentration of SH^- in the cooking liquor was calculated as B-value/m_{CL}. Four portions of 10 g of cooking liquor were analyzed and the average value was taken.

The amount of cooking liquor required to obtain the desired concentrations, i.e $[OH^-]$, $[SH^-]$ = 0.26 mol/kg cooking liquor, was calculated by Equation A.2.

$$c_1 \cdot v_1 = c_2 \cdot v_2 \tag{A.2}$$

Where index 1 = current concentration of cooking liquor and index 2 = desired concentration of cooking liquor. c_1 = current concentration of SH^-, v_1 = amount of cooking liquor required, c_2 = 0.26 mol/kg and v_2 = 1000 g,

The amount of water required to obtain a total volume of 1000 g was then calculated according to Equation A.3.

$$v_{water} = 1000 - v_1 \tag{A.3}$$

B

Cell wall thickness distribution

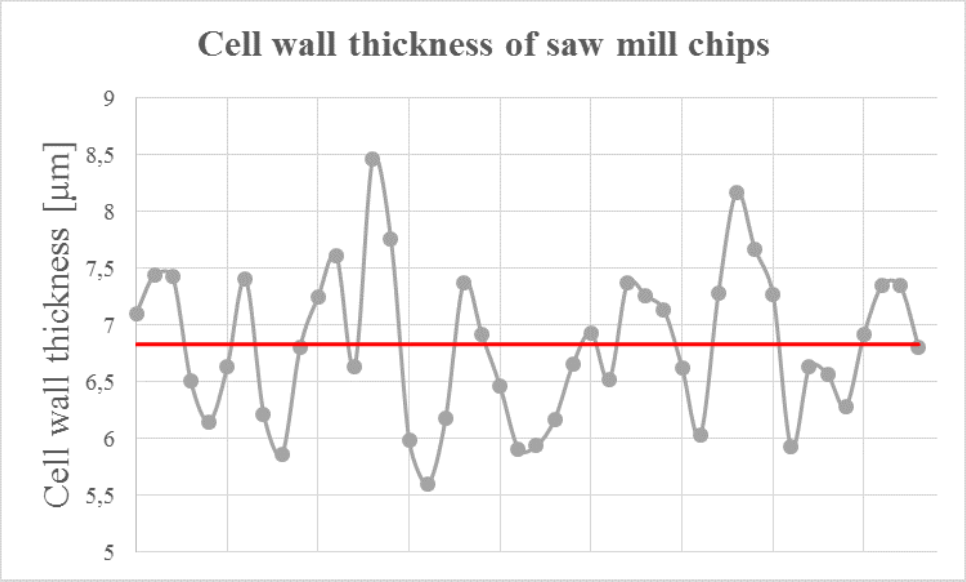

Figure B.1: Distribution of the cell wall thickness measured. The red line indicates the average cell wall thickness [µm]

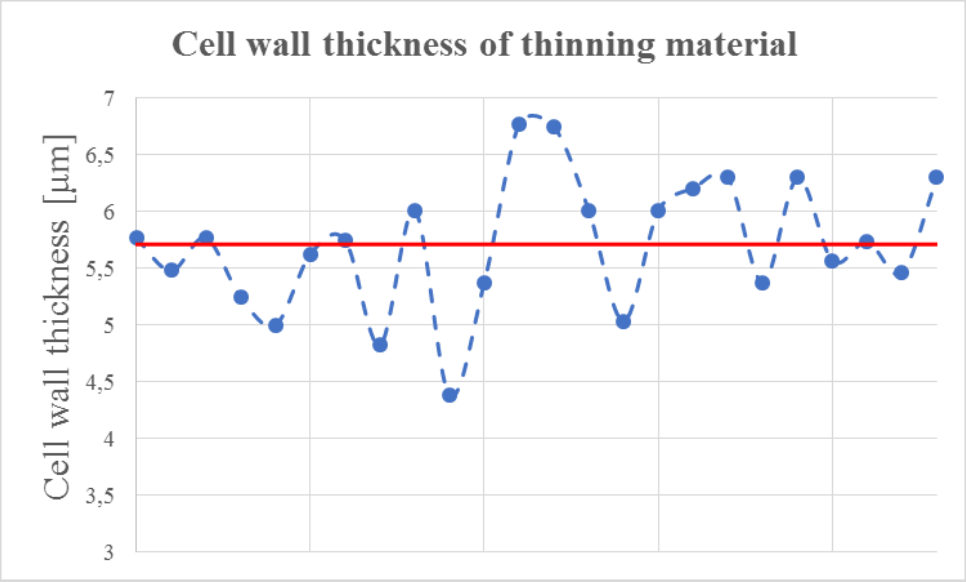

Figure B.2: Distribution of the cell wall thickness measured. The red line indicates the average cell wall thickness [µm]

C

Calculating the amount of cellulose and hemicellulose

Using the information about the monosugars quantity, the amount of cellulose and hemicellulose can be calculated according to Equation C.1-C.3 below (Wigell et al. 2007).

$$Cellulose = Glu - \frac{1}{3.5}Man \tag{C.1}$$

$$Galactoglucomannan = Gal + (1 + \frac{1}{3.5})Man \tag{C.2}$$

$$Xylan = Xyl + Ara + (4 - O - MeGlcA + HexA) \tag{C.3}$$

In Equation C.1-C.3, Glu = glucose, Man= mannose, Gal = galactose, Xyl = xylose, Ara = arabinose, 4-O-MeGlcA = 4-O-Methyl glucuronic acid and HeXA=hexenuronic acid.

D
MWD

The MWD was computed from the raw data obtained using a MATLAB-script created by Anders Ahlbom and Anders Åkersjö 2019, see Figure D.1-D.11. The molecular weight (M) in kDa was calculated from running time (t) in minutes using the calibration curve, see Equation D.1.

$$M = 10^{10.427816-(0.214092 \cdot t/60)}/1000 \tag{D.1}$$

The response was normalized according to Equation D.2, where x is the response.

$$\text{Normalised response} = \frac{x - x_{min}}{x_{max} - x_{min}} \tag{D.2}$$

The x-axis displays the molecular weight in kDa and the y-axis the normalised response.

D.1 Thinning Material

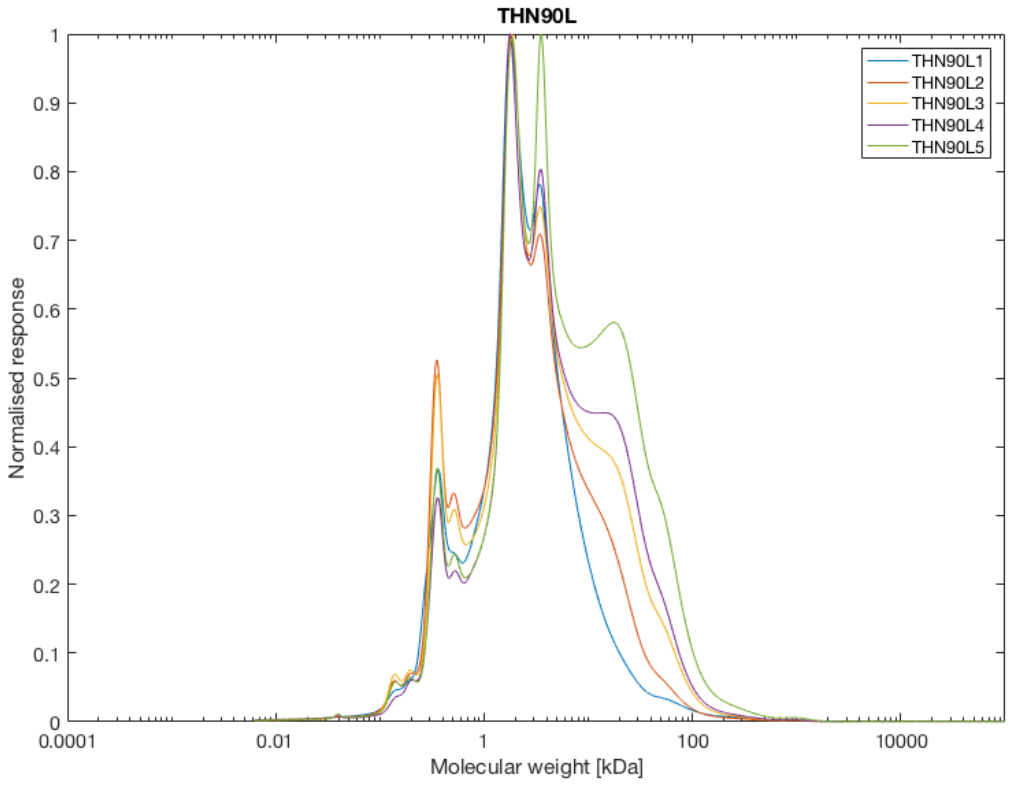

Figure D.1: MWD Thinning Material 90 minutes, 148°C

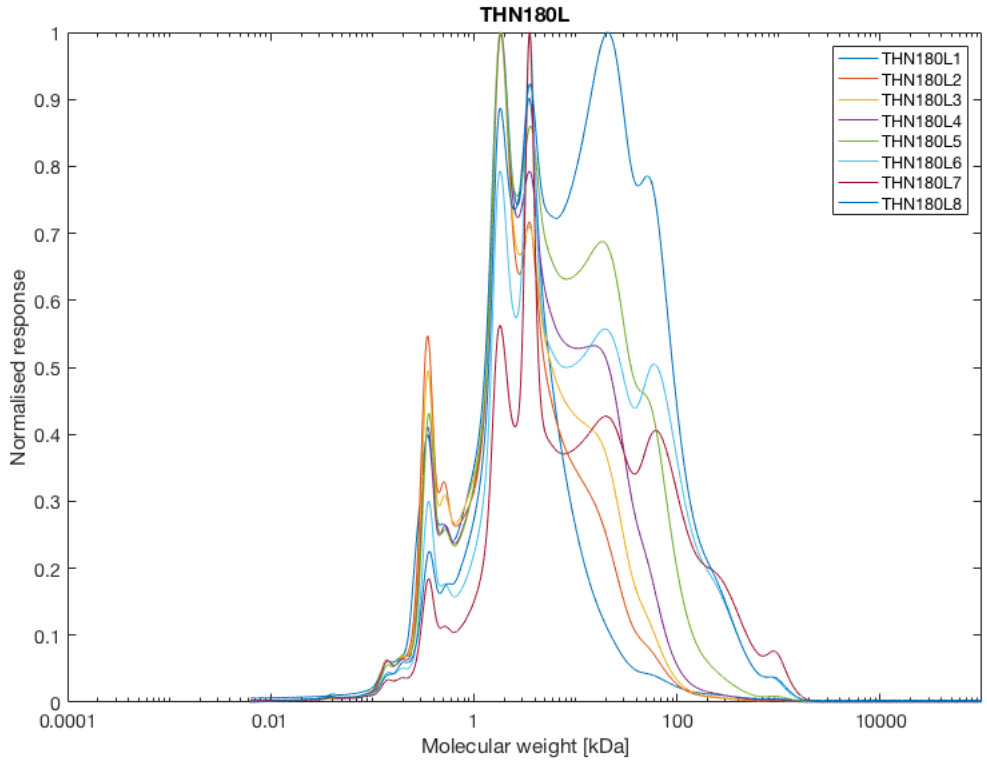

Figure D.2: MWD Thinning Material 180 minutes, 148°C

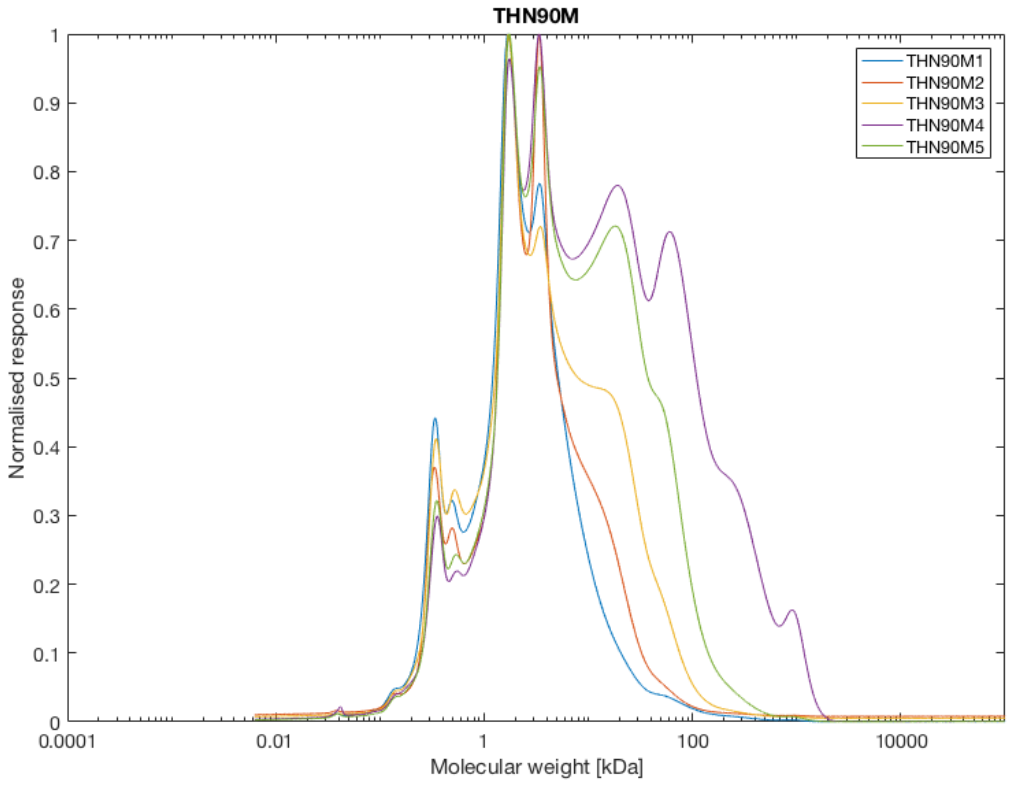

Figure D.3: MWD Thinning Material 90 minutes 158°C

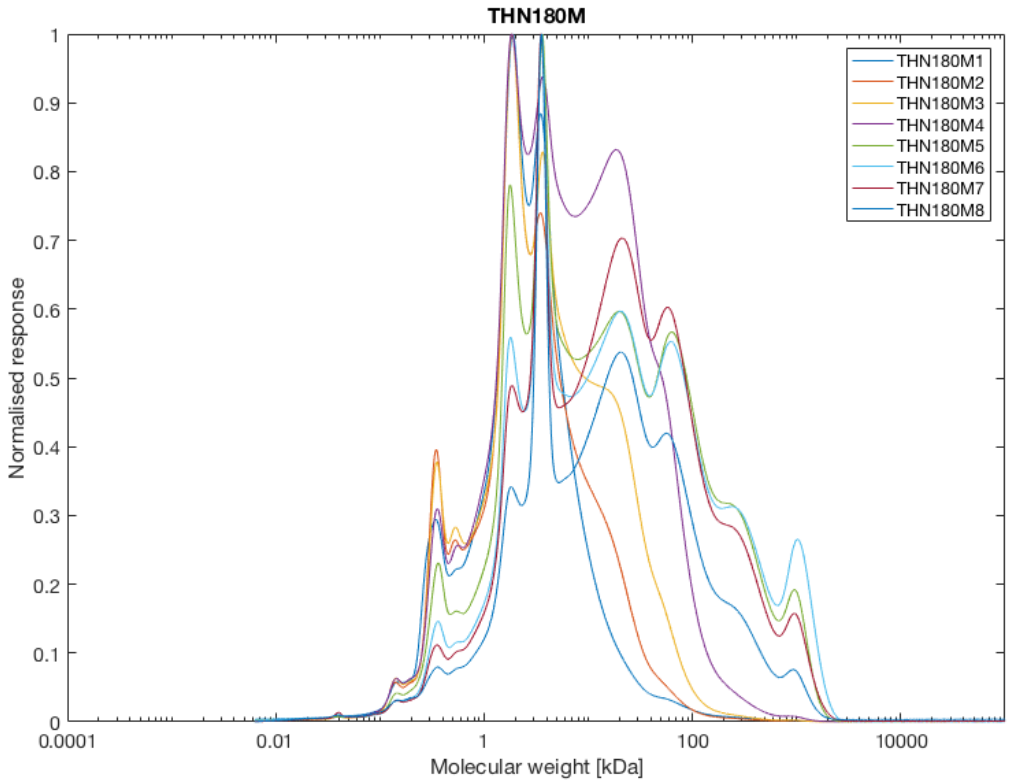

Figure D.4: MWD Thinning Material 180 minutes 158°C

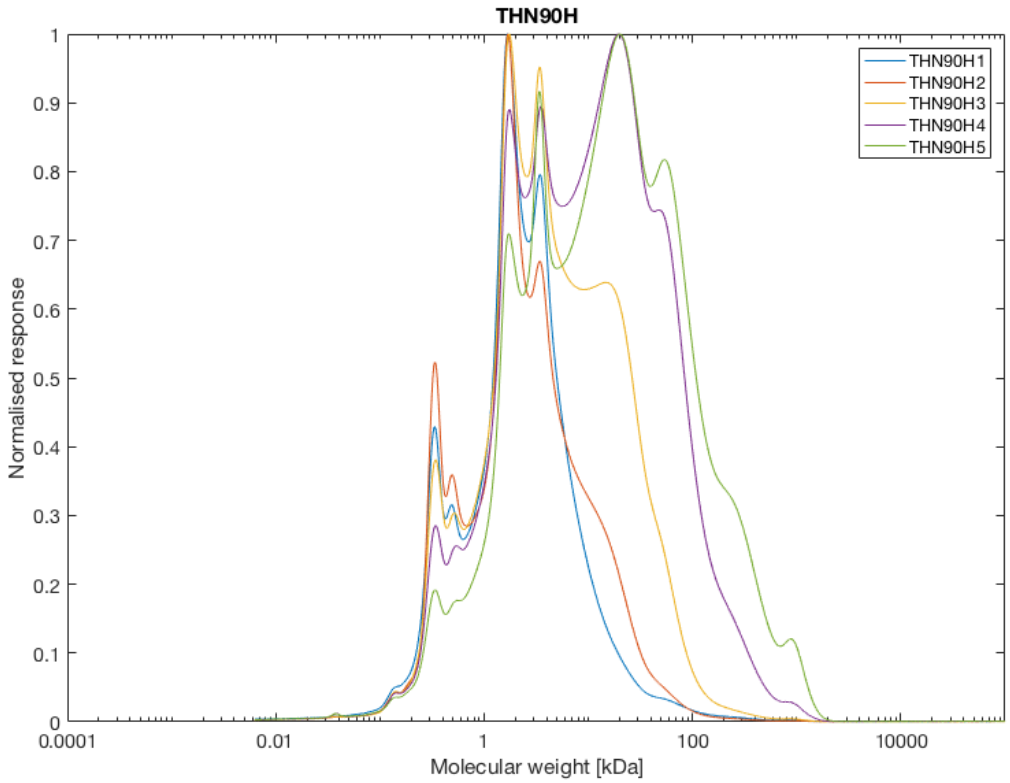

Figure D.5: MWD Thinning Material 90 minutes 168°C

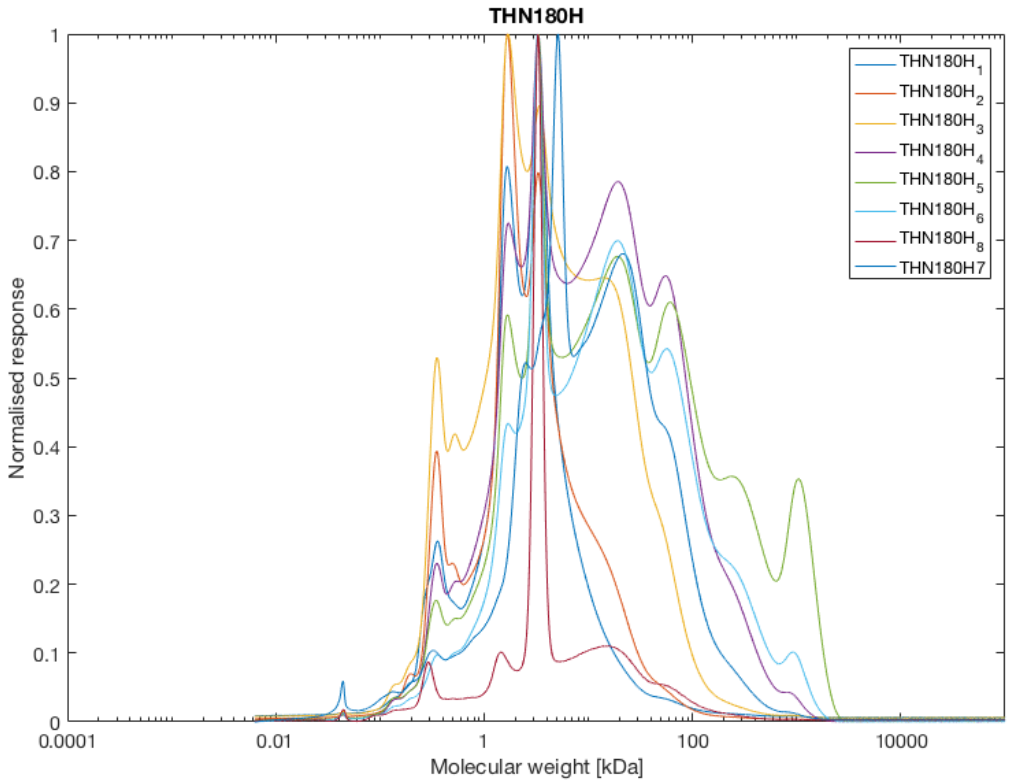

Figure D.6: MWD Thinning Material 180 minutes 168°C

Sample 7 was prepared by adding DMSO directly to the filter with PL and was let to stay over day to drip through.

D.2 Sawmill chips

No sample for SGV90L was taken.

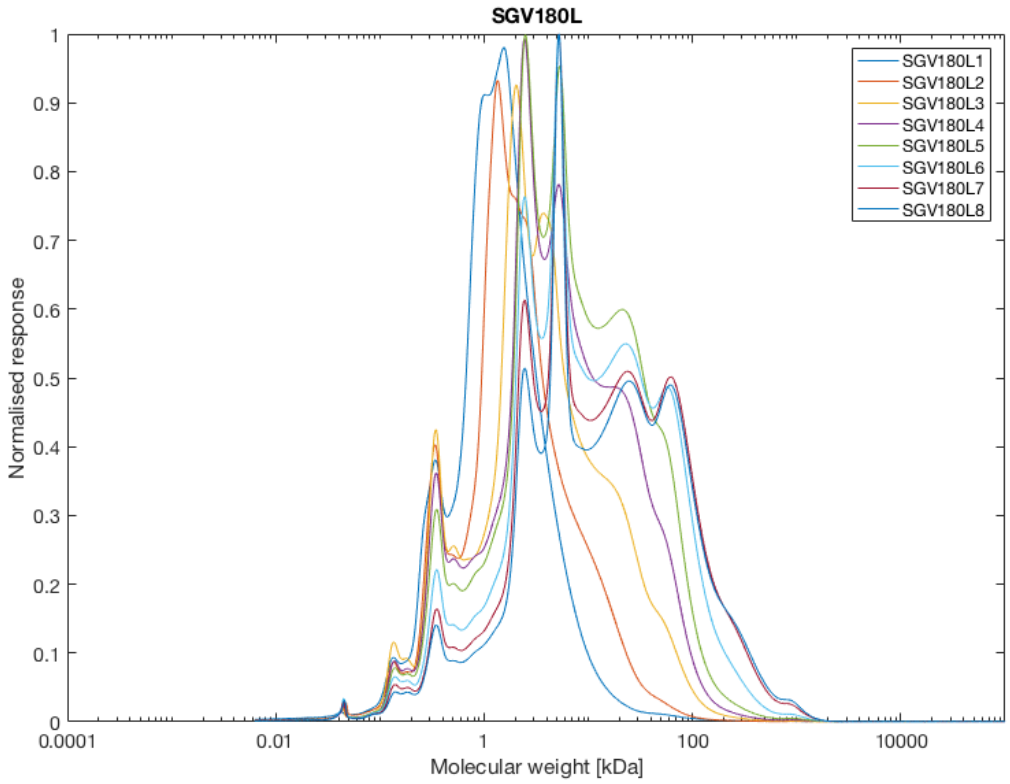

Figure D.7: MWD sawmill chips 180 minutes, 148°C

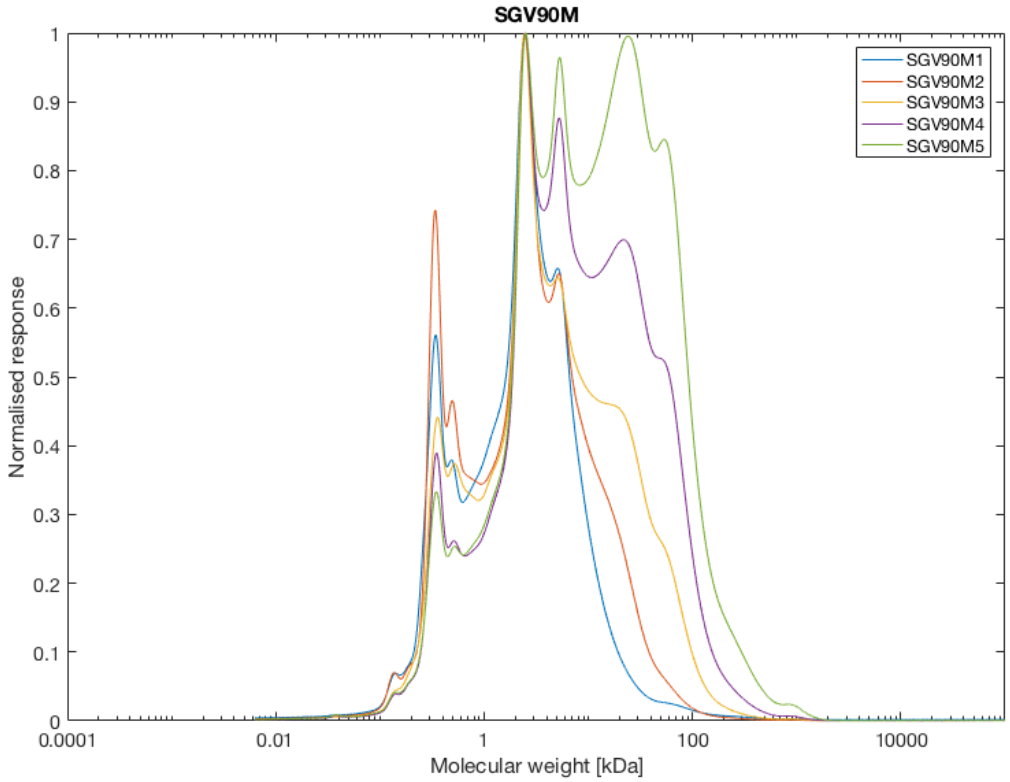

Figure D.8: MWD sawmill chips 90 minutes, 158°C

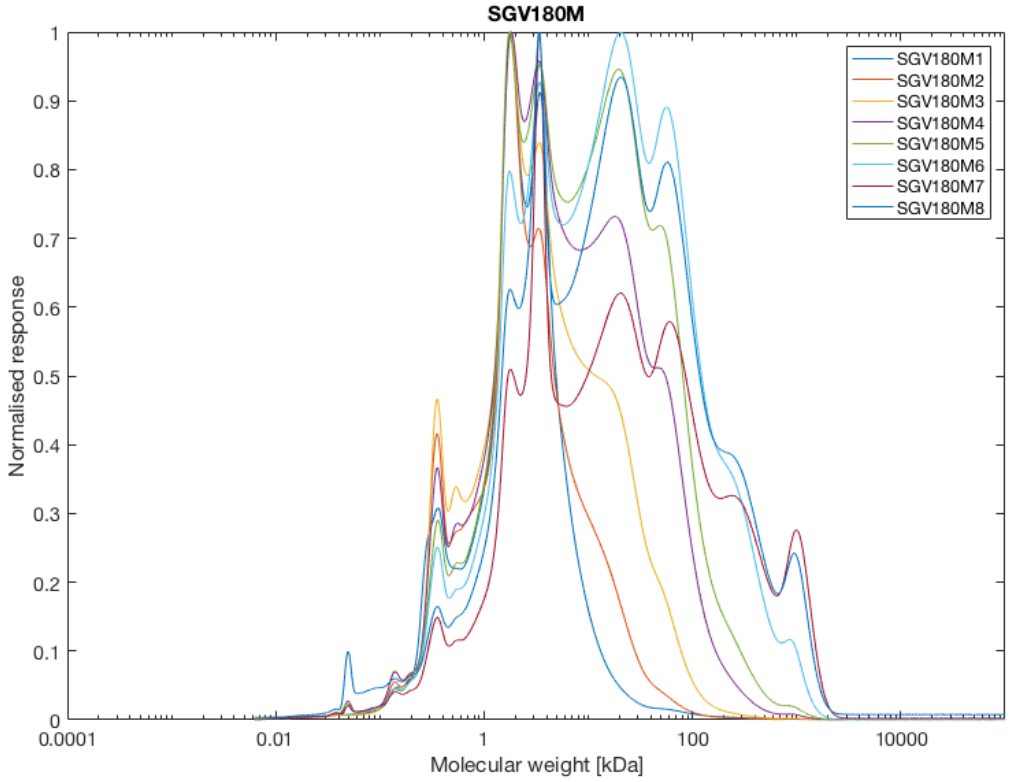

Figure D.9: MWD sawmill chips 180 minutes, 158°C

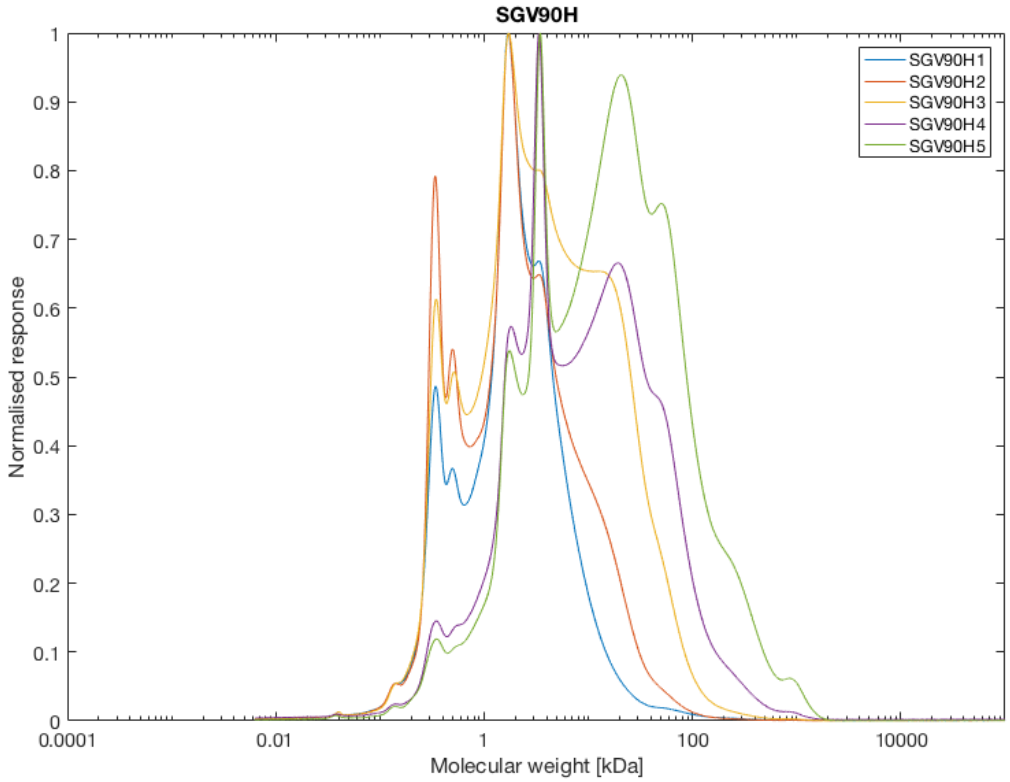

Figure D.10: MWD sawmill chips 90 minutes, 168°C

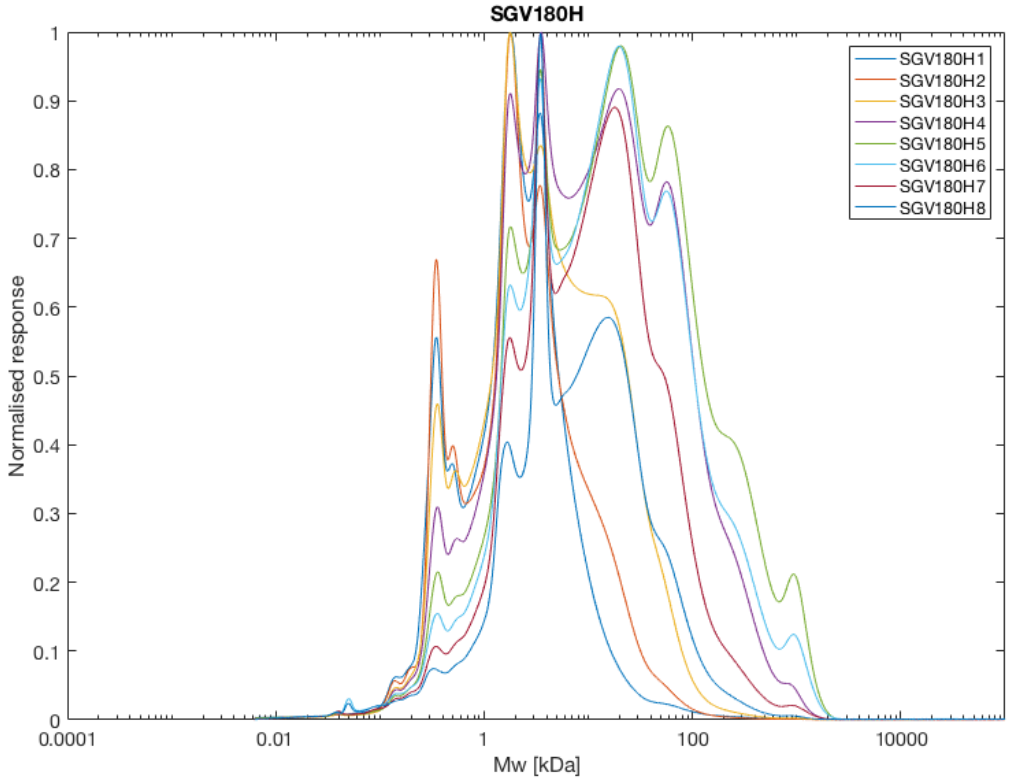

Figure D.11: MWD sawmill chips 180 minutes, 168°C

E

Klason lignin in pulp

The content of klason lignin in the pulp at various times expressed as percentage of the initial klason lignin in the wood meal, was calculated using an average of forward and backward balances.

The forward balance was calculated based on the knowledge of the KL in the wood meal and subtracting the KL in the BL frations, according to Equation E.1-E.9.

$$\text{KL in pulp in sample 0} = \frac{\text{KL in WM}}{\text{KL in WM}} \tag{E.1}$$

$$\text{KL in pulp in sample 1} = \frac{\text{sample 0 - KL in BL fraction 1}}{\text{KL in WM}} \tag{E.2}$$

$$\text{KL in pulp in sample 2} = \frac{\text{sample 1 - KL in BL fraction 2}}{\text{KL in WM}} \tag{E.3}$$

$$\text{KL in pulp in sample 3} = \frac{\text{sample 2 - KL in BL fraction 3}}{\text{KL in WM}} \tag{E.4}$$

$$\text{KL in pulp in sample 4} = \frac{\text{sample 3 - KL in BL fraction 4}}{\text{KL in WM}} \tag{E.5}$$

$$\text{KL in pulp in sample 5} = \frac{\text{sample 4 - KL in BL fraction 5}}{\text{KL in WM}} \tag{E.6}$$

$$\text{KL in pulp in sample 6} = \frac{\text{sample 5 - KL in BL fraction 6}}{\text{KL in WM}} \tag{E.7}$$

$$\text{KL in pulp in sample 7} = \frac{\text{sample 6 - KL in BL fraction 7}}{\text{KL in WM}} \tag{E.8}$$

$$\text{KL in pulp in sample 8} = \frac{\text{sample 7 - KL in BL fraction 8}}{\text{KL in WM}} \tag{E.9}$$

The backward balance was calculated based on the knowledge of KL in the final pulp and adding the KL in the BL fractions, according to Equation E.18-E.10.

$$\text{KL in pulp in sample 8} = \frac{\text{KL in pulp}}{\text{KL in WM}} \tag{E.10}$$

$$\text{KL in pulp in sample 7} = \frac{\text{sample 8 + BL fraction 8}}{\text{KL in WM}} \tag{E.11}$$

$$\text{KL in pulp in sample 6} = \frac{\text{sample 7 + BL fraction 7}}{\text{KL in WM}} \tag{E.12}$$

$$\text{KL in pulp in sample 5} = \frac{\text{sample 6 + BL fraction 6}}{\text{KL in WM}} \tag{E.13}$$

$$\text{KL in pulp in sample 4} = \frac{\text{sample 5 + BL fraction 5}}{\text{KL in WM}} \tag{E.14}$$

$$\text{KL in pulp in sample 3} = \frac{\text{sample 4 + BL fraction 4}}{\text{KL in WM}} \tag{E.15}$$

$$\text{KL in pulp in sample 2} = \frac{\text{sample 3 + BL fraction 3}}{\text{KL in WM}} \tag{E.16}$$

$$\text{KL in pulp in sample 1} = \frac{\text{sample 2 + BL fraction 2}}{\text{KL in WM}} \tag{E.17}$$

$$\text{KL in pulp in sample 0} = \frac{\text{sample 1 + BL fraction 1}}{\text{KL in WM}} \tag{E.18}$$

F

Calculating the amount of sugar acids

The amount of acids formed during 0-90 minutes is calculated as the difference between the sugar content of the wood meal and the sugar content of the total sugar content of BL+pulp at 90 minutes, according to Equation F.1. The content of acids during the later part of the cook is calculated according to Equation F.2.

$$m_{\text{Acid 0-90}} = m_{\text{sugar in WM}} - (m_{\text{sugar in pulp90}} + m_{\text{sugar in BL fraction 1-5}}) \tag{F.1}$$

$$m_{\text{Acid 90-180}} = m_{\text{sugar in pulp90}} - (m_{\text{sugar in pulp180}} + m_{\text{sugar in BL fraction 6-8}}) \tag{F.2}$$